SKI Rapport 98:19

# Pourbaix diagrams for the system copper-chlorine at 5–100 °C

Björn Beverskog
Studsvik Material AB
S-611 82 Nyköping, Sweden

Ignasi Puigdomenech
Studsvik Eco & Safety AB
S-611 82 Nyköping, Sweden

April 1998

# List of contents

# Abstract

Pourbaix diagrams for the copper-chlorine system in the temperature interval 5–100 °C have been revised. Predominance diagrams for dissolved copper containing species have also been calculated. Two different total concentrations of each dissolved element, $10^{-4}$ and $10^{-6}$ molal for copper and 0.2 and 1.5 molal for chlorine have been used in the calculations.

Chloride is the predominating chlorine species in aqueous solutions. Presence of chloride increases the corrosion regions of copper at the expense of the immunity and passivity regions in the Pourbaix diagrams. $CuCl_2 \cdot 3Cu(OH)_2$ is the only copper-chloride solid phase that forms at the concentrations of chlorine studied. However, its stability area decreases with increasing temperature. The ion $CuCl_2^-$ predominates at all temperatures at $[Cl(aq)]_{tot} = 0.2$ molal and this reduces the immunity and passivity areas. A corrosion region exists between the immunity and passivity regions at 100 °C at $[Cu(aq)]_{tot} = 10^{-6}$ and $[Cl(aq)]_{tot} = 0.2$ molal. At the chlorine concentration of 1.5 molal the corrosion region exists in the whole temperature range investigated. The ion $CuCl_3^{2-}$ predominates at 5-25 and 100 °C, while $CuCl_2^-$ predominates at 50-80 °C at $[Cl(aq)]_{tot} = 1.5$ molal. A copper concentration of $10^{-4}$ molal reduces the corrosion areas due to expansion of the immunity and passivity areas. However, a corrosion region still exists between the immunity and passivity regions at all investigated temperatures at $pH_T < 9.5$ and 1.5 molal chloride concentration.

According to our calculations the copper canisters in the deep nuclear waste repository should not corrode at the copper concentration of $10^{-6}$ molal and the chloride concentration of 0.2 molal. However, at 80-100 °C the equilibrium potentials postulated for the Swedish nuclear repository are dangerously close to a corrosion situation. According to our calculations the copper canisters in the Swedish repository corrode at 80-100 °C at the chloride concentration of 1.5 molal.

# Sammanfattning

Pourbaix-diagram (potential/pH-diagram) för systemet koppar-klor vid 5-100 °C har reviderats. Predominansdiagram för lösta specier innehållande koppar har också beräknats. Två olika koncentrationer av lösta specier har använts i beräkningarna: $10^{-4}$ och $10^{-6}$ molal för koppar samt 0.2 och 1.5 molal för klor.

Klorid är den predominerande klorspecien i akvatiska lösningar. Närvaro av klorid ökar området för korrosion av koppar på bekostnad av immun- (ingen korrosion *per* definition) och passivområdet (låg korrosionshastighet) i Pourbaix-diagrammen. $CuCl_2 \cdot 3Cu(OH)_2$ är den enda fasta koppar-kloridfas som bildas vid dessa halter av klor, men dess stabilitetsområde minskar med ökande temperatur. Jonen $CuCl_2^-$ predominerar vid alla temperaturer vid $[Cl(aq)]_{tot} = 0.2$ molal och detta reducerar såväl immun- som passivområdet. Ett korrosionsområde existerar mellan immun- och passivområdet vid 100 °C och $[Cu(aq)]_{tot} = 10^{-6}$ och $[Cl(aq)]_{tot} = 0.2$ molal. En kloridhalt på 1.5 molal medför att ett korrosionsområde mellan immun- och passivområdet existerar i hela det undersökta temperaturområdet. Jonen $CuCl_3^{2-}$ predominerar vid 5-25 och 100 °C, medan $CuCl_2^-$ predominerar vid 50-80 °C vid $[Cl(aq)]_{tot} = 1.5$ molal. En kopparkoncentration på $10^{-4}$ molal reducerar korrosionsområdena eftersom immun- och passivområdena expanderar. Trots detta existerar fortfarande ett korrosionsområde mellan immun- och passivområdet vid $pH_T < 9.5$ och 1.5 molal kloridhalt.

Enligt våra beräkningar skall kopparbehållare i det djupa slutförvaret inte korrodera vid kopparhalten $10^{-6}$ molal och kloridhalten 0.2 molal. Men, vid 80-100 °C är slutförvarets postulerade potentialer farligt nära en korrosionssituation. Enligt våra beräkningar korroderar kopparbehållarna i det tänkta slutförvaret vid 80-100 °C vid kloridhalten 1.5 molal.

# 1 Introduction

The spent nuclear fuel in Sweden will be encapsulated into composite canisters, according to the KBS-3 concept developed by SKB[1]. The duplex container consists of an outer copper canister and an inner of carbon steel. Copper is chosen due to its excellent corrosion resistance and carbon steel for its mechanical properties. The thickness of the copper layer is 5 cm.

The canisters will be placed deep down in granitic bedrock (500 m) and embedded in a buffer of compacted bentonite. The temperature at the canister surface will have an initial maximum of ~ 80 °C, due to the heat produced by the spent nuclear fuel. Whether the radiation level is high enough to produce radiolysis of water at the copper surface is not yet fully clear.

The groundwater circulating in the fractures of the bedrock surrounding the repository will contain chloride, among other anions. The concentration of chloride can vary from diluted to concentrated.

To predict the corrosion behavior of a metal from thermodynamic calculations it is essential to consider all the species that the metal can form with the components of the environment. As copper has a strong affinity for chloride several solid phases and aqueous complexes can form. It is particularly important to include the dissolved species in thermodynamic calculations for Pourbaix diagrams since they decide the size of the corrosion areas in the diagram.

Pourbaix diagrams for the copper-chlorine system have been published by Pourbaix (1945) and Duby (1977). Pourbaix diagrams for the copper-chloride system have been reported by Mattsson (1962), Pourbaix (1973), Skrifvars (1993), Ahonen (1995), and Nila and González (1996). Only Ahonen presented diagrams for elevated temperatures (100 °C). The concentrations of chlorine/chloride used in these studies were 0.035 to 1 M. The choice of species of previous works are shown in **Table 1**. The work of Nila and González is not considered as $NH_3$ was included and unit copper concentration were used. Most previous publications on Pourbaix diagrams for the aqueous copper-chlorine system contain two solid copper-chloride phases, with the exception of Duby and Ahonen, see **Table 1**.

The aim of the present work is to revise the Pourbaix diagrams for the system of copper-chlorine at elevated temperatures as well as low temperatures (which have not been reported before). This work is based on a previous study of the Pourbaix diagrams for copper (Beverskog and Puigdomenech, 1995). Further studies are intended to include sulfur and carbonate into the system, which will better simulate the expected repository for spent nuclear fuel. The thermodynamic calculations for copper in different aquatic environments will also be used to simulate the corrosion behavior of copper canisters in the expected environment of the Swedish final repository for spent nuclear fuel.

**Table 1**. *Copper-chloride species included in previously published Pourbaix diagrams.*

| **Species** | Pourbaix (1945) | Mattson (1962) | Pourbaix (1973) | Duby (1977) | Skrifvars (1993) | Ahonen (1995) |
|---|---|---|---|---|---|---|
| *Solids* | | | | | | |
| CuCl | x | x | x | x | x | |
| $CuCl_2$ | | | | x | x | |

[1]SKB: Swedish Nuclear Fuel and Waste Management Co.

| | | | | | | |
|---|---|---|---|---|---|---|
| $CuCl \cdot Cu(OH)_3$ | | x | | | | |
| $CuCl_2 \cdot 2H_2O$ | x | | | x | | |
| $CuCl_2 \cdot Cu(OH)_2$ | | | | x | | |
| $CuCl_2 \cdot 2Cu(OH)_2$ | | | | x | | |
| $CuCl_2 \cdot 3Cu(OH)_2$ | | | x | x | | |
| $3CuCl_2 \cdot 7Cu(OH)_2$ | | | | x | | |
| | | | | | | |
| *Dissolved* | | | | | | |
| $CuCl(aq)$ | | | | | | x |
| $CuCl_2^-$ | x | x | | x | | x |
| $CuCl_3^{2-}$ | | x | | x | x | x |
| $CuCl_4^-$ | | | | | | |
| $Cu_2Cl_4^{2-}$ | | | | | | x |
| $Cu_3Cl_6^{3-}$ | | | | | | x |
| $CuCl^+$ | | x | | x | x | x |
| $CuCl_2(aq)$ | | x | | x | | x |
| $CuCl_3^-$ | | x | | x | | x |
| $CuCl_4^{2-}$ | | x | | x | | x |
| $CuCl_2OH^{2-}$ | | | | | | x |
| $CuClOH^-$ | | | | | | x |
| $CuCl(OH)_2^{2-}$ | | | | | | x |
| | | | | | | |
| $\Sigma$(s + aq) | 2 + 1 = 3 | 2 + 6 =8 | 2 + 0 = 2 | 7 + 6 =13 | 2 + 2 = 4 | 0 + 12 = 12 |

# 2 Choice of species

It is of fundamental importance which species (solid phases, fluids, aqua ions, and aqua complexes) are included in the thermodynamic calculations in a given chemical system. Some species are not stable in water solutions while others can only form at high temperatures or at extreme compositions. It is therefore necessary to critically evaluate the species which are expected to exist in a system before they are allowed to be the basis for the thermodynamic calculations. Calculations based on wrong species give misleading information on chemical equilibria.

## 2.1 Chlorine - water

Chlorine has the electron configuration [Ne] $3s^2\ 3p^5$, *i.e.* 5 p-electrons outside a full 3s shell and a noble gas shell. The large electronegativity of chlorine makes it easy to form anions. The noble gas shell is formed by addition of an electron, which leads to the common oxidation state -I. Chlorine forms positive oxidation numbers in compounds with oxygen, as the latter is more electronegative, resulting in chlorine oxidation numbers +I to +VII, with the exception of +II. However, the most common oxidation state of chlorine in aqueous solutions is -I, which is chloride.

Seven species (six dissolved and one gaseous) have been included in the chlorine - water system, **Table 2**. As seen from the Gibbs free energy values chloride, is the most stable of the chlorine species

**Table 2**
Thermodynamic data at 25 °C for the system chlorine-water

| | $\Delta_f G°$ | $S°$ | $C_p\,(T)/(J{\cdot}K^{-1}{\cdot}mol^{-1}) = a + bT + cT^{-2}$ | | |
|---|---|---|---|---|---|
| Specier | $(kJ{\cdot}mol^{-1})$ | $(J{\cdot}K^{-1}{\cdot}mol^{-1})$ | $a^{\dagger}$ | $b \times 10^3$ | $c \times 10^{-6}$ |
| $Cl_2(g)$ | 0 | 223.08 | 46.956 | –4.0158 | $0^{\ddagger}$ |
| $Cl^-$ | –131.2 | 56.60 | –123.18 | | |
| $ClO^-$ | –37.67 | 42.00 | –205.9 | | |
| HClO(aq) | –80.02 | 142.0 | –72.0 | | |
| $ClO_2^-$ | –10.25 | 101.3 | –127.61 | | |
| $HClO_2(aq)$ | –0.940 | 188.3 | 6.4 | | |
| $Cl_2(aq)$ | 6.94 | 121 | 45 | | |

†: For aqueous ions and complexes "*a*" corresponds to the standard partial molar heat capacity at 25 °C, and its temperature dependence has been calculated with the revised Helgeson-Kirkham-Flowers model as described in the text.

‡: $C_p°\,(Cl_2(g), T) / (J{\cdot}K^{-1}{\cdot}mol^{-1}) = a + bT + cT^{-2} + dT^2 + eT^{0.5}$, with $d = 9.93 \times 10^{-7}$ and $e = -2.05 \times 10^2$.

## 2.2 Copper - water

The choice of species and thermodynamical data for the copper-water system has been discussed elsewhere (Beverskog and Puigdomenech, 1995). 13 copper containing species (4 solids and 9 aqueous) have been included in the calculations, **Table 3**.

**Table 3**
Thermodynamic data at 25 °C for the system copper-water

| Specier | $\Delta_f G°$ (kJ·mol$^{-1}$) | $S°$ (J·K$^{-1}$·mol$^{-1}$) | $C_p(T)$/(J·K$^{-1}$·mol$^{-1}$) = $a + bT + cT^{-2}$ $a$† | $b \times 10^3$ | $c \times 10^{-6}$ |
|---|---|---|---|---|---|
| Cu(cr) | 0 | 33.15 | 20.531 | 8.611 | 0.155 |
| $Cu_2O$(cr) | –147.90 | 92.36 | 58.199 | 23.974 | –0.159 |
| CuO(cr) | –128.29 | 42.6 | 48.597 | 7.427 | –0.761 |
| $Cu(OH)_2$(cr) | –359.92 | 87.0 | 86.99 | 23.26 | –0.54 |
| $Cu^+$ | 48.87 | 40.6 | 57.3 | | |
| CuOH(aq) | –122.32 | 226 | –280 | | |
| $Cu(OH)_2^-$ | –333.05 | –135 | 562 | | |
| $Cu^{2+}$ | 65.04 | –98.0 | –23.8 | | |
| $CuOH^+$ | –126.66 | –61 | 382 | | |
| $Cu(OH)_2$(aq) | –316.54 | 26 | 214 | | |
| $Cu(OH)_3^-$ | –493.98 | –14 | 105 | | |
| $Cu(OH)_4^{2-}$ | –657.48 | –175 | 800 | | |
| $Cu_2(OH)_2^{2+}$ | –285.1 | –4 | 190 | | |
| $Cu_3(OH)_4^{2+}$ | –633.0 | –59 | 404 | | |

†: For aqueous ions and complexes "$a$" corresponds to the standard partial molar heat capacity at 25 °C, and its temperature dependence has been calculated with the revised Helgeson-Kirkham-Flowers model as described in the text.

## 2.3 Copper - chlorine - water

Nine species (two solids and seven dissolved) containing copper-chlorine species have been included in the aqueous system of copper-chloride, **Table 4**.

The complex $CuClOH^-$ was reported by Sugasaka and Fujii (1976) in 5 M $NaClO_4$ solutions at 25 °C. The existence of this species has not been verified by any other source. Furthermore, the data at 250 °C by Var'yash and Rekharskiy (1981) that was explained by these authors with the formation of $CuClOH^-$ can also be modeled in a satisfactory way by assuming the formation of $CuCl_2^-$ and $CuCl_3^{2-}$ only. Therefore, $CuClOH^-$ is not included in the calculations presented here.

**Table 4**
Thermodynamic data at 25 °C for the system copper-chlorine-water

| | $\Delta_f G°$ | $S°$ | $C_p(T)/(J\cdot K^{-1}\cdot mol^{-1})$ $= a + bT + cT^{-2}$ | | |
|---|---|---|---|---|---|
| Specier | $(kJ\cdot mol^{-1})$ | $(J\cdot K^{-1}\cdot mol^{-1})$ | $a^\dagger$ | $b \times 10^3$ | $c \times 10^{-6}$ |
| CuCl(cr) | −121.3 | 88.4 | 38.28 | 34.98 | |
| $CuCl_2 \cdot 3Cu(OH)_2$(s) | −1339.5 | 370.3 | 336 | | |
| CuCl(aq) | −94.3 | 277 | −760 | | |
| $CuCl_2^-$ | −246.0 | 214.8 | −175 | | |
| $CuCl_3^{2-}$ | −373.4 | 215.3 | 0 | | |
| $CuCl^+$ | −69.83 | −1 | 73 | | |
| $CuCl_2$(aq) | −200.83 | 104 | 130 | | |
| $CuCl_3^-$ | −327.5 | 169 | 227 | | |
| $CuCl_4^{2-}$ | −452.42 | 237 | −775 | | |

†: For aqueous ions and complexes "*a*" corresponds to the standard partial molar heat capacity at 25 °C, and its temperature dependence has been calculated with the revised Helgeson-Kirkham-Flowers model as described in the text.

# 3 Thermochemical data

A critical review of published thermodynamic data has been performed for the solids and aqueous species described in previous Sections. Data is usually available only for a reference temperature of 25 °C in the form of standard molar Gibbs free energy of formation from the elements ($\Delta_f G°$), standard molar entropy ($S°$), and standard molar heat capacity ($C_p°$). The standard *partial* molar properties are used for aqueous species. Extrapolation of these data to other temperatures is performed with the methodology described later in the "Calculations" section. Missing entropy and heat capacity values for copper species and compounds at 25 °C have been estimated as described below in this Section. The data selected for the calculations performed in this report are summarized in **Tables 3** and **4**. Values for entropy (and enthalpy) changes selected in different studies depend on the equations used for the temperature variation of $C_p°$ for aqueous solutes, and therefore, some of the $S°$ values selected here differ substantially from those in other compilations, as discussed below.

Auxiliary data for chlorine, and its aqueous species, has been retrieved from the USGS report by Robie *et al.* (1978), the NBS compilation of Wagman *et al.* (1982), CODATA's key values by Cox *et al.* (1989), the NEA uranium review by Grenthe *et al.* (1992), and the $C_p°$ values given in papers by Shock and Helgeson (1988 and 1989).

## 3.1 Solids

The standard Gibbs free energy of formation and entropy for CuCl(cr) (nantokite) is that selected by Whang *et al.* (1997), while the heat capacity data is that reported in Kubaschewski *et al.* (1993). For atacamite ($CuCl_2 \cdot 3Cu(OH)_2$(cr)) the data is that of King *et al.* 1973, except for the heat capacity, which has been estimated with the methods given in Kubaschewski *et al.* (1993). It should be noted that the standard Gibbs free energy of formation of atacamite seems to originate from the solubility study of Näsänen and Tamminen (1949).

## 3.2 Aqueous species

The thermodynamic properties of $H_2O(l)$ at 25 °C recommended by CODATA (Cox *et al.*, 1989) have been used in this work. The temperature dependence of these properties has been calculated with the model of Saul and Wagner (1989). The dielectric constant of water (which is needed for the revised Helgeson-Kirkham-Flowers model described below) has been obtained with the equations given by Archer and Wang (1990).

The $\Delta_f G°$ value for CuCl(aq) has been obtained from the equilibrium constant reported by Ahrland and Rawsthorne (1970) extrapolated from 5 M $NaClO_4$ to $I$=0 with the specific ion interaction equations given in Appendix D of Grenthe *et al.* (1992). The $S°$ value for CuCl(aq) was obtained from the $T$-dependence of the equilibrium constant of formation for this complex as reported by Crerar and Barnes (1976). CuCl(aq) is a minor species which has a large uncertainty in its thermodynamic data, and does not predominate in the any of the Pourbaix diagrams presented here.

$\Delta_f G°$ and $S°$ values for $CuCl_2^-$ and $CuCl_3^{2-}$ are those recommended by Whang *et al.* (1997). The $C_p°$ data has been obtained from the $T$-dependence of the equilibrium constants in Var'yash (1992) for $CuCl_2^-$, while for $CuCl_3^{2-}$ a $C_p°$ value was obtained by analogy with the chloride complexes of silver(I) studied by Seward (1976).

$\Delta_f G°$ and $S°$ values for $CuCl^+$ and $CuCl_2(aq)$ are those recommended by Whang *et al.* (1997). Corresponding values for $CuCl_3^-$ and $CuCl_4^{2-}$ are difficult to obtain because these weak complexes are only formed at high concentrations of chloride ion. The high $[Cl^-]$ values result in significant changes in the activity coefficients during the experiments. Extrapolation of the thermodynamic data to standard conditions (zero ionic strength) will depend largely on the methodology used to estimate the effects of the changing ionic media on equilibrium constants and enthalpies of reaction. Furthermore, the effects of changing background electrolyte concentrations and those of complex formation are mathematically highly correlated. This results in large uncertainties associated with thermodynamic data of weak complexes at standard conditions. In general, strong physical evidence from a variety of experimental techniques is often required to establish un-equivocally the existence and strength of weak complexes.

For $CuCl_3^-$ and $CuCl_4^{2-}$ the equilibrium constants given by Ramette (1986) have been used to derive $\Delta_f G°$ values, while standard entropies have been obtained from estimated enthalpy changes (in $kJ \cdot mol^{-1}$):

| | | |
|---|---|---|
| $Cu^{2+} + Cl^- \rightleftarrows CuCl^+$ | $\Delta_r H° = 8.4$ | (Whang *et al.*, 1997) |
| $Cu^{2+} + 2\ Cl^- \rightleftarrows CuCl_2(aq)$ | $\Delta_r H° = 23$ | - " - |
| $Cu^{2+} + 3\ Cl^- \rightleftarrows CuCl_3^-$ | $\Delta_r H° = 30$ | Estimated |
| $Cu^{2+} + 4\ Cl^- \rightleftarrows CuCl_4^{2-}$ | $\Delta_r H° = 40$ | Estimated |

It should be pointed out that the relatively large uncertainties in the standard values for $CuCl_3^-$ and $CuCl_4^{2-}$ do not affect the results of the present study, because of the restricted range of chloride concentrations it involves.,

The $C_p°$ data for all four chloride complexes of Cu(II) has been obtained by analogy with the zinc(II) system using the $\Delta_r C_p°$ values reported by Ruaya and Seward (1986).

# 4 Calculations

The methods and assumptions to calculate equilibrium diagrams have been described elsewhere (Beverskog and Puigdomenech, 1995 and 1996). The technique to draw Pourbaix diagrams have also been presented by Beverskog and Puigdomenech (1995). Pourbaix diagrams have been drawn with computer software (Puigdomenech, 1983) using the chemical compositions calculated with the SOLGASWATER algorithm (Eriksson, 1979), which obtains the chemical composition of systems with an aqueous solution and several possible solid compounds by finding the minimum of the Gibbs free energy of the system.

The ionic strength for the calculations corresponding to each coordinate in the diagrams has been calculated iteratively from the electroneutrality condition: on acid solutions a hypothetical anion has been ideally added to keep the solutions neutral and on alkaline solutions a cation has been added. This hypothetical components have been taken into account when calculating the value of the ionic strength.

The values for the activity coefficient, $\gamma_i$, of a given aqueous ion, $i$, have been approximated with a function of the ionic strength and the temperature:

$$\log \gamma_i = - z_i^2 A \sqrt{I} / (1 + B \, å \, I) - \log (1+0.0180153 \, I) + b \, I$$

where $I$ is the ionic strength, $A$, $B$, and $b$ are temperature-dependent parameters, $z_i$ is the electrical charge of the species $i$, and $å$ is a "distance of closest approach", which in this case is taken equal to that of NaCl ($3.72 \times 10^{-10}$ m). This equation is a slight modification of the model by Helgeson *et al.*, (see Eqs. 121, 165-167, 297, and 298 in Helgeson *et al.* (1981); and Eqs. 22 and 23 in Oelkers and Helgeson (1990)). The values of $A$, $B$, and $b$ at a few temperatures are:

| $T$ / °C | $p$ / bar | $A$ | $B$ | $b$ |
|---|---|---|---|---|
| 25 | 1.000 | 0.509 | 0.328 | 0.064 |
| 100 | 1.013 | 0.600 | 0.342 | 0.076 |
| 150 | 4.76 | 0.690 | 0.353 | 0.065 |
| 200 | 15.5 | 0.810 | 0.367 | 0.046 |
| 250 | 39.7 | 0.979 | 0.379 | 0.017 |
| 300 | 85.8 | 1.256 | 0.397 | –0.029 |

For neutral aqueous solutions, it has been approximated that their activity coefficients are unity at all values of ionic strength and temperature. This would have negligible effects on the calculated Pourbaix diagrams.

The effect of the activity corrections for higher ion strength was observable on the diagrams compared to those calculated at I=0. For example the ion $CuCl^+$ does not show up in the corrected diagrams, while it does at I=0. Furthermore, the stability of the solid phase $CuCl_2 \cdot 3Cu(OH)_2$ is reduced in the corrected version, and the predominance area of the uncharged complex $Cu(OH)_2(aq)$ is also affected.

Calculations to draw the diagrams presented in this work have been performed for five temperatures in the interval 5-10 °C (5, 25, 50, 80, and 100), which covers adequately the temperature range which copper

canisters will experience in the expected environment of the Swedish final repository for spent nuclear fuel. Calculations have been performed at two total concentrations of dissolved copper species $10^{-4}$ and $10^{-6}$ molal (mol/kg of water) combined with two concentrations of chloride 0.2 and 1.5 molal. Because they are temperature-independent, molal concentration units are used in the calculations.

The parallel sloping dashed lines in the Pourbaix diagrams given in the **Appendix** limit the stability area of water at atmospheric pressure of gaseous species. The upper line represents the oxygen equilibrium line ($O_2(g)/H_2O(l)$) and potentials above this line will oxidize water with oxygen evolution. The lower line represents the hydrogen line ($H^+/H_2(g)$) and potentials below this line will result in hydrogen evolution.

*All values of pH given in this work are values at the specified temperature. The temperature dependence* for the ion product of water,

$$H_2O(l) \rightleftarrows H^+ + OH^-$$

changes the neutral pH value of pure water with the temperature (neutral environment = 1/2 $pK_{w,T}$). To facilitate reading the Pourbaix diagrams in the **Appendix**, the neutral pH value for the temperature of each diagram is given as a vertical dotted line.

# 5 Results and discussion

Two general remarks can be concluded regarding the temperature and concentration dependence of the diagrams. Firstly, temperature affects the different stability areas of immunity, passivity and corrosion. The immunity area (stability of the metal itself) decreases with increasing temperature. The passivity area (solid compounds) is almost temperature independent. With increasing temperature the corrosion area at acidic pH changes due to a slight decrease of the passivity area and a decrease of the immunity area, while the corrosion area at alkaline pH increases (it is shifted to lower pH values). The reason for this behavior is related to the temperature dependence of the ion product of water. Secondly, the concentration of dissolved metallic species also changes the different stability areas. The immunity and passivity areas increase with increasing concentration at increasing temperature, while the corrosion areas decrease.

The Pourbaix diagrams for the system chlorine -water at the total concentration of 0.2 molal are shown in **Figs. 1A-E**. Two aqueous ions and a dissolved gas show up in the diagrams. The chloride ion ($Cl^-$) predominate in a large area and covers the stability area of water. The chlorite ion ($ClO_2^-$) predominates at high potentials outside the stability area of water. Chlorine gas ($Cl_2$) shows up in strong acidic solutions at high potentials. A higher concentration of chlorine (1.5 molal) does not change the diagrams compared to 0.2 molal, except for minimal changes (almost not seen in this scale used in the diagrams) of the equilibrium lines and are therefore not shown here.

*$[Cu(aq)]_{tot} = 10^{-6}$ molal and $[Cl(aq)]_{tot} = 0.2$ molal*

The results from the thermodynamic calculations for the aqueous system of copper-chlorine are summarized in the Pourbaix diagrams with varied concentrations of dissolved copper and chlorine, **Figs. 2-7**. The Pourbaix diagrams for the copper-chlorine system at [Cu(aq)] = $10^{-6}$ molal and [Cl(aq)] = 0.2 molal are shown in **Figs. 2A-E**. The presence of chlorine decreases both the immunity area of copper and the passivity area of $Cu_2O$ calculated in Beverskog and Puigdomenech (1995) due to the aqueous complex $CuCl_2^-$. At higher potentials the solid $CuCl_2 \cdot 3Cu(OH)_2$ forms at the expense of the stability area of CuO. Increasing temperature reduces the immunity area as well as the passivity areas of $Cu_2O$ and $CuCl_2 \cdot 3Cu(OH)_2$. The former is not stable at 100 °C and the latter at T > 5 °C. The size of the stability area of CuO is less temperature dependent.

Due to the lack of stability of $Cu_2O$ at 100 °C a corrosion region exists between the immunity and passivity areas at this temperature. This is caused by the relatively high ion strength in the solution. At zero ionic strength this situation does not occur (Fig. 10E in Beverskog and Puigdomenech, 1995).

$CuCl_2^-$ is the only copper-chloride species that appears in the predominance diagram for dissolved species, **Figs. 3A-E**.

Copper canister in the Swedish deep repository environment will probably not corrode at 0.2 molal concentration of chloride. But the redox potential for the equilibria $Cu/CuCl_2^-$ is –200 $mV_{SHE}$ at 80 °C and –260 $mV_{SHE}$ at 100 °C, is dangerously close to the anticipated redox potential range in the repository (-300 to -400 $mV_{SHE}$). The situation is pH-independent at pH < 9.8. At higher pH copper canisters corrode. Lower temperatures increase the redox potential for the $Cu/CuCl_2^-$ equilibria and therefore decreasing temperatures are beneficial for the safety of the copper canisters.

$CuCl_2^-$ is the predominating dissolved copper species in the deep repository environment.

*$[Cu(aq)]_{tot} = 10^{-6}$ molal and $[Cl(aq)]_{tot} = 1.5$ molal*

The Pourbaix diagrams for the copper-chloride system at [Cu(aq)] = $10^{-6}$ molal and a higher chloride concentration [Cl(aq)] = 1.5 molal are visualized in **Figs. 4A-E.** Independent of the temperature no $Cu_2O$ forms, which results in a corrosion region between the immunity and passivity areas. The immunity area and the passivity area of $CuCl_2 \cdot 3Cu(OH)_2$ decreases with temperature and the latter is not stable at temperatures above 50 °C. The ion $CuCl^+$ forms at high potentials in acidic solutions at 100 °C.

$CuCl_3^{2-}$ predominates at 5-25 and 100 °C in the predominating diagram for dissolved species, **Figs 5A, B** and **E.** $CuCl_2^-$ predominates at 50 and 80 °C, **Figs. 5C** and **D.** The uncharged copper(II) chloride complex $CuCl_2(aq)$ predominates at 50-100 °C.

Copper canisters in the Swedish repository environment corrodes (according to our calculations) at the anticipated temperatures of 80-100 °C and potential range. However, decreasing temperatures increase the redox potential equilibria for $Cu/CuCl_2^-$ or $CuCl_3^{2-}$ and therefore the redox potential will fall in the immunity region of copper, indicating no corrosion.

$CuCl_3^{2-}$ is the predominating aqueous copper-chloride species at 5-25 and 100 °C in the deep repository environment. $CuCl_2^-$ is the predominating aqueous copper-chloride species at 50-80 °C.

*$[Cu(aq)]_{tot}$ = $10^{-4}$ molal and $[Cl(aq)]_{tot}$ = 0.2 molal*

The Pourbaix diagrams for the copper-chloride system at a higher copper concentration ($10^{-4}$ molal) and [Cl(aq)] = 0.2 molal are shown in **Figs. 6A-E.** Increasing copper concentration increases the immunity and the passivity areas for copper and reduces the corrosion areas. The solid copper-chloride compound $CuCl_2 \cdot 3Cu(OH)_2$ becomes stable in the whole temperature interval.

Predominance diagrams of dissolved copper species are the same as those in **Figs. 3A-E.**

The copper canisters in the repository will not corrode in an environment of $[Cu(aq)]_{tot} = 10^{-4}$ molal and $[Cl(aq)]_{tot} = 0.2$ molal.

$CuCl_2^-$ is the predominating aqueous copper-chloride species in the deep repository environment.

*$[Cu(aq)]_{tot}$ = $10^{-4}$ molal and $[Cl(aq)]_{tot}$ = 1.5 molal*

The Pourbaix diagrams for the copper-chloride system at a high copper concentration ($10^{-4}$ molal) and a high chloride concentration [Cl(aq)] = 1.5 molal are visualized in **Figs. 7A-E.** The diagrams are very similar to those in **Fig. 2** with the exception that the immunity and passivity areas are larger.

For predominance diagrams of dissolved copper species under these conditions are the same as those in **Figs. 5A-E.**

Copper canisters in the deep Swedish repository corrode at 80-100 °C according to our calculations under these conditions. $CuCl_3^{2-}$ is the predominating aqueous copper-chloride species at 5-25 and 100 °C in the deep repository environment. $CuCl_2^-$ is the predominating aqueous copper-chloride species at 50-80 °C.

The Pourbaix diagrams published by Ahonen (1995) are calculated at the chloride concentrations $10^{-2}$ and 1 molal and the copper concentrations of $10^{-7}$ molal. The redox potential was given in electron activity (pE), but to directly compare those diagrams with present work we recalculated on diagrams in the pE-scale at 25 and 100 °C. pE is calculated to the redox potential by

$$pE = E_{SHE} \quad F/RTln10$$

Where F and R are the Faraday and Rydbergs gas constant, T is in degrees Kelvin. At 25 °C, $pE = E_{SHE} / 0.059$ V

However, the agreement is satisfactory.

# 6 Conclusions

The following points summarize the results of the thermodynamic calculations performed in this work:

- The Pourbaix diagram for the copper-chloride system at 5 °C is shown for the first time.
- $CuCl_2 \cdot 3Cu(OH)_2(cr)$ has a stability that decreases with increasing temperature.
- $CuCl_2^-$ predominates in all diagrams of $[Cl(aq)]_{tot} = 0.2$ molal and thereby reduces the immunity and passivity areas of copper.
- A corrosion region exists between the immunity and passivity areas at 100 °C at $[Cu(aq)]_{tot} = 10^{-6}$ molal and $[Cl(aq)]_{tot} = 0.2$ molal.
- The corrosion region exists at 5-100 °C $[Cl(aq)] = 1.5$ molal.
- $CuCl_3^{2-}$ predominates at 5-25 and 100 °C, while $CuCl_2^-$ forms at 50-80 °C at $[Cl(aq)]_{tot} = 1.5$ molal.
- $CuCl_2(aq)$ predominates at 50-100 °C and $[Cl(aq)]_{tot} = 1.5$ molal.
- $CuCl^+$ have a small area of predominance at 100 °C at $[Cl(aq)]_{tot} = 1.5$ molal.
- The copper concentration of $[Cu(aq)]_{tot} = 10^{-4}$ m reduces the corrosion areas in the system due to the expansion of the immunity and passivity regions. However, at the chloride concentration of 1.5 molal there still exists a corrosion region between the immunity and passivity regions.
- The copper canisters in the deep repository do not corrode according to our calculations at the copper concentration of $10^{-6}$ molal and the chloride concentration of 0.2 molal. However, at 80-100 °C the calculated equilibrium potentials are dangerously close to a corrosion situation.
- The copper canisters corrode at 80-100 °C at the chloride concentration of 1.5 molal in the repository environment at the expected pH-values and redox potentials.

# Acknowledgments

Thanks are due to S.-O. Pettersson for running several of the computer calculations.

# References

Ahonen, L. (1995). Chemical stability of copper canisters in deep repository. Report YJT 95-19, Nuclear Waste Commission of Finnish Power Companies.

Ahrland, S. and Rawsthorne, J. (1970). The stability of metal halide complexes in aqueous solution. VII. The chloride complexes of copper(I). *Acta Chem. Scand.*, **24**, 157-172.

Archer, D.G. and Wang, P. (1990). The dielectric constant of water and Debye-Hückel limiting law slopes. *J. Phys. Chem. Ref. Data*, **19**, 371-411.

Beverskog, B. and Puigdomenech, I. (1995). SITE-94. Revised Pourbaix diagrams for copper at 5-150 °C, SKI Report 95:73, Swedish Nuclear Power Inspectorate, Stockholm, Sweden.

Beverskog, B. and Puigdomenech, I. (1996). Revised Pourbaix diagrams for iron at 25–300 °C. *Corrosion Sci.*, **38**, 2121-2135.

Cox, J. D., Wagman, D. D., and Medvedev, V. A. (1989). *CODATA key values for thermodynamics.* Hemisphere Publ. Co., New York.

Crerar, D. A., and Barnes, H. L. (1976). Ore solution chemistry V. Solubilities of chalcopyrite and chalcocite assemblages in hydrothermal solution at 200° to 350°C, *Econ. Geol.*, **71**, 772-794.

Duby, P. (1977). *The Thermodynamic Properties of Aqueous Inorganic Copper systems.* INCRA Monograph IV. The Metallurgy of Copper. Int. Copper Res. Ass..

Eriksson, G. (1979). An algorithm for the computation of aqueous multicomponent, multiphase equilibria. *Anal. Chim. Acta*, **112**, 375-383.

Grenthe, I., Fuger, J., Konings, R. J. M., Lemire, R. J., Muller, A. B., Nguyen-Trung, C., and Wanner, H. (1992). *Chemical thermodynamics of uranium.* Elsevier Sci. Publ., Amsterdam.

Helgeson H.C., Kirkham, D.H. and Flowers, G.C. (1981). Theoretical prediction of the thermodynamic behaviour of aqueous electrolytes at high pressures and temperatures: IV. Calculation of activity coefficients, osmotic coefficients, and apparent molal and standard and relative partial molal properties to 600°C and 5 kb, *Amer. Jour. Sci.*, **281**, 1249-1516.

King, E. G., Mah, A. D., and Pankratz, L. B. (1973) *Thermodynamic properties of copper and its inorganic compounds*, The International Copper Research Association (INCRA), New York.

Kubaschewski, O., Alcock, C. B., and Spencer, P. J. (1993) *Materials thermochemistry.* Pergamon Press, Oxford, 6th edition.

Mattsson, E (1962) Potential-pH diagram för korrosionsstudier. Med beräkningsexempel avseende systemet Cu-Cl-$H_2O$. *Svensk Kemisk Tidskrift*, **74**, 76-88.

Nilas, C and González, Thermodynamics of Cu-$H_2SO_4$-$Cl^-$-$H_2O$ and Cu-$NH_4Cl$-$H_2O$ based on predominance-existance diagrams and Pourbaix-type diagrams, *Hydrometallurgy*, **42** (1996) 63.

Näsänen, R., and Tamminen, V. (1949) The equilibria of cupric hydroxysalts in mixed aqueous solutions of cupric and alkali salts at 25°, *J. Am. Chem. Soc.*, **71**, 1994–1998.

Nila, C. and González, I. (1996). Thermodynamics of Cu-$H_2SO_4$-$Cl^-$-$H_2O$ and Cu-$NH_4Cl$-$H_2O$ based on predominance-existence diagrams and Pourbaix-type diagrams, *Hydrometallurgy*, **42**, 63-82.

Oelkers, E.H. and Helgeson, H.C. (1990) Triple-ion anions and polynuclear complexing in supercritical electrolyte solutions, *Geochim. Cosmochim. Acta*, **54**, 727-738.

Pourbaix, M. (1945). *Thermodynamique des Solutions Aqueuses Diluées. Représentation Graphique du Role du pH et du Potentiel. Ph. D. Thesis. Université Libredes Bruxelles,*. Engl. transl. : (1965) *Thermodynamics in Dilute Aqueous Solutions, with Applications to Electrochemistry and Corrosion*, Arnold, London.

Pourbaix, M. (1973). *Lectures on Electrochemical Corrosion.* Plenum Press, New York-London, p. 121-142.

Puigdomenech, I. (1983). INPUT, SED and PREDOM: computer programs drawing equilibrium diagrams. Technical Report TRITA-OOK-3010, Dept. Inorg. Chem., The Royal Institute of Technology, 100 44 Stockholm, Sweden.

Ramette, R. W. (1986). Copper(II) complexes with chloride ion, *Inorg. Chem.*, **25**, 2481–2482.

Robie, R. A., Hemingway, B. S., and Fisher, J. R. (1978). Thermodynamic properties of minerals and related substances at 298.15 K and 1 bar ($10^5$ Pascals) pressure and at higher temperatures, USGS Bull. 1452.

Ruaya, J. R. and Seward, T. M. (1986). The stability of chlorozinc(II) complexes in hydrothermal solutions up to 350°C, *Geochim. Cosmochim. Acta*, **50**, 651–661.

Saul, A. and Wagner, W. (1989). A fundamental equation for water covering the range from the melting line to 1273 K at pressures up to 25 000 MPa. *J. Phys. Chem. Ref. Data*, **18**, 1537–1564.

Seward, T. M. (1976). The stability of chloride complexes of silver in hydrothermal solutions up to 350°C, *Geochim. Cosmochim. Acta*, **40**, 1329–1341.

Shock, E. L. and Helgeson, H. C. (1988). Calculation of the thermodynamic and transport properties of aqueous species at high pressures and temperatures: correlation algorithms for ionic species and equation of state predictions to 5 kb and 1000°C. *Geochim. Cosmochim. Acta*, **52**, 2009–2036. *Errata*: **53** (1989) 215.

Shock, E. L., Helgeson, H. C., and Sverjensky, D. A. (1989). Calculation of the thermodynamic and transport properties of aqueous species at high pressures and temperatures: standard partial molal properties of inorganic neutral species. *Geochim. Cosmochim. Acta*, **53**, 2157–2183.

Skrifvars, B. (1993). Metal Pourbaix diagrams in complexing environments. The use of thermodynamic stability diagrams for predicting corrosion behavoiur of metals. *Progress in Understanding and Prevention of Corrosion*, Vol.1, Barcelona, Spain, July 1993, p. 437-446.

Sugasaka, K. and Fujii, A. (1976). A spectrophotometric study of copper(I) chlorocomplexes in aqueous 5 M Na($Cl,ClO_4$) solutions, *Bull. Chem. Soc. Japan*, **49**, 82-86.

Var'yash, L. N. (1992) Cu(I) complexing in NaCl solutions at 300 and 350°C, *Geochem. Int.*, **29**, 84-92.

Var'yash, L. N. and Rekharskiy, V. I. (1981). Behaviour of Cu(I) in chloride solutions, *Geochem. Int.*, **18**, 61-67.

Wagman, D. D., Evans, W. H., Parker, V. B., Schumm, R. H., Halow, I., Bailey, S. M., Churney, K. L., and Nuttall, R. L. (1982). The NBS tables of chemical thermodynamic properties: Selected values for inorganic and $C_1$ and $C_2$ organic substances in SI units. *J. Phys. Chem. Ref. Data*, **11**, Suppl. No. 2, 1–392.

Wang, M., Zhang, Y., and Muhammed, M. (1997). Critical evaluation of thermodynamics of complex formation of metal ions in aqueous systems. III. The system Cu(I,II)-$Cl^-$-e at 298.15 K, *Hydrometal.*, **45**, 653-672.

# Appendix: Diagrams

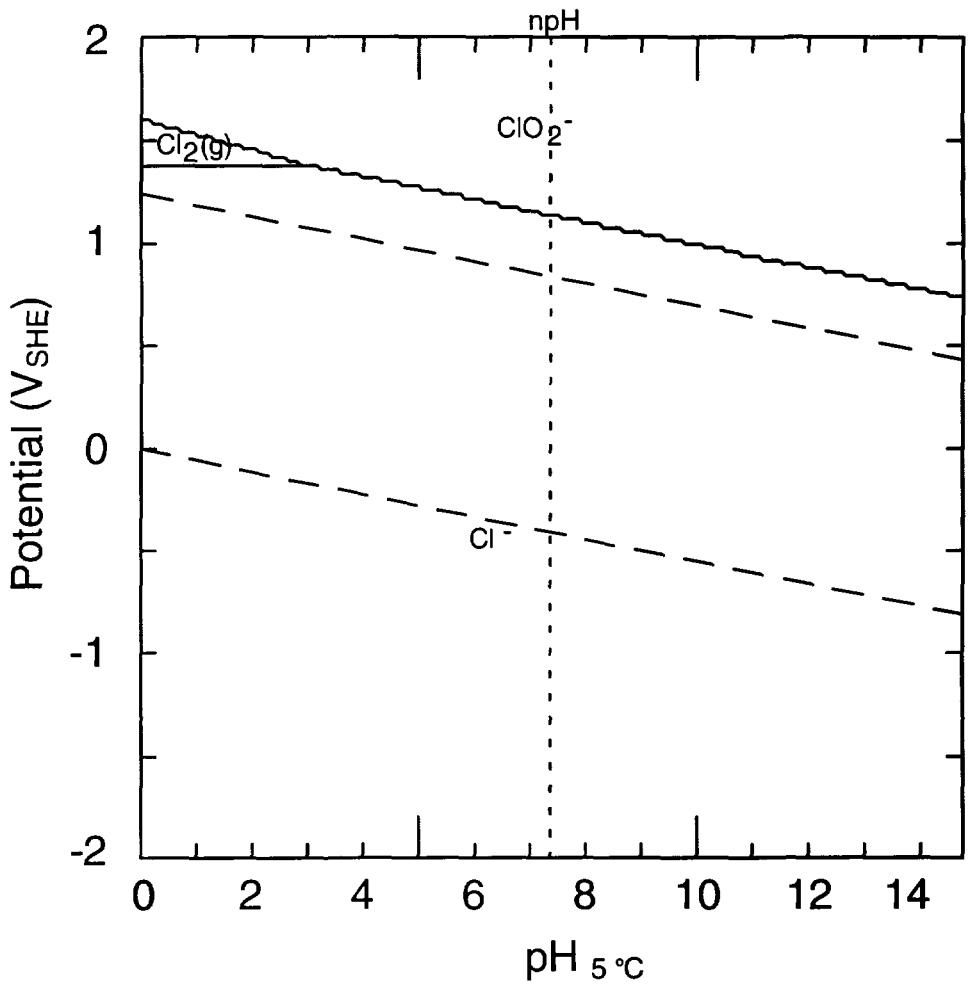


**Figure 1A**
Pourbaix diagram for chlorine at 5 °C and $[Cl(aq)]_{tot}$ = 0.2 molal.

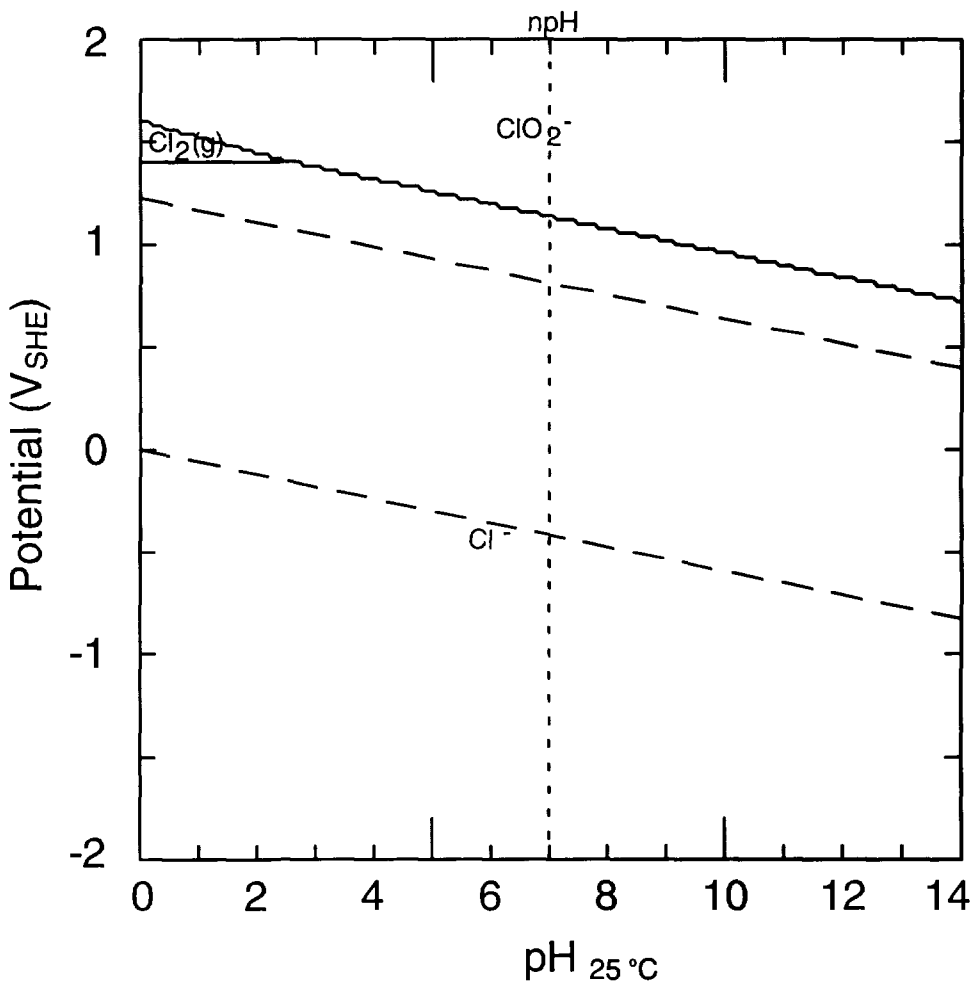


**Figure 1B**
Pourbaix diagram for chlorine at 25 °C and $[Cl(aq)]_{tot}$ = 0.2 molal.

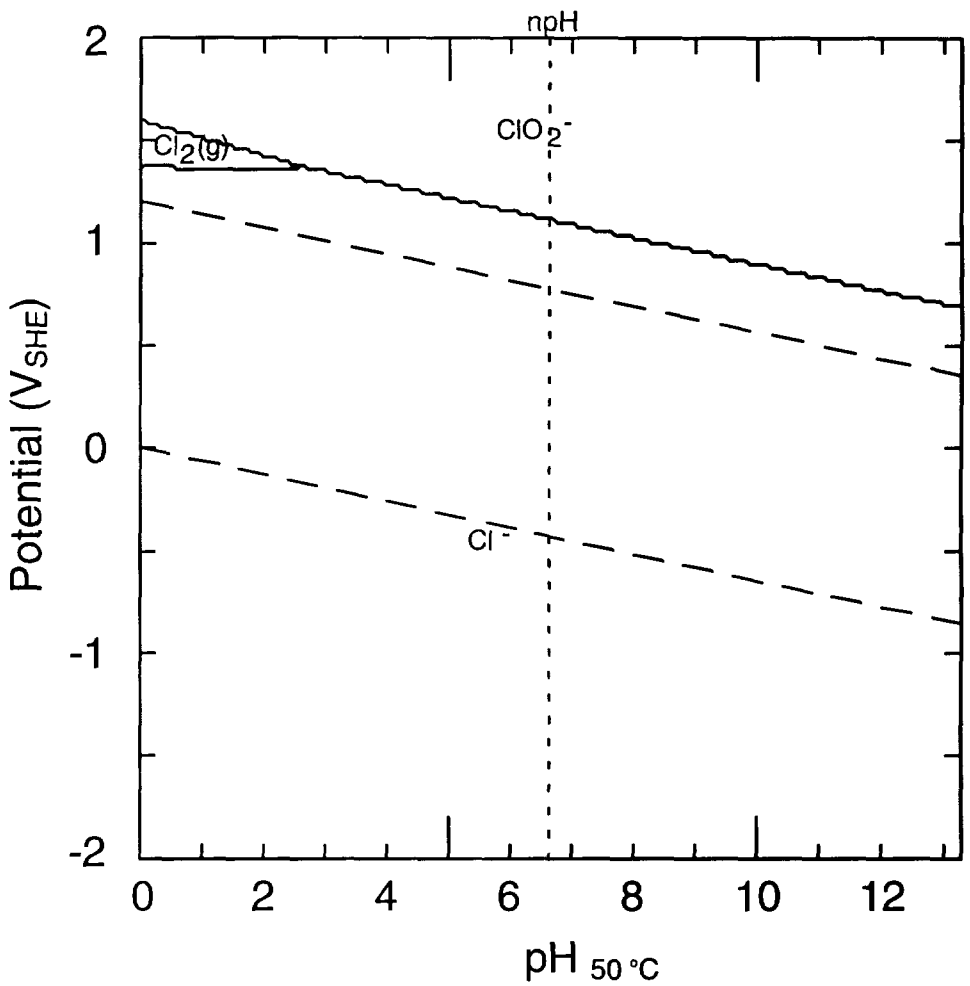


**Figure 1C**
Pourbaix diagram for chlorine at 50 °C and $[Cl(aq)]_{tot}$ = 0.2 molal.

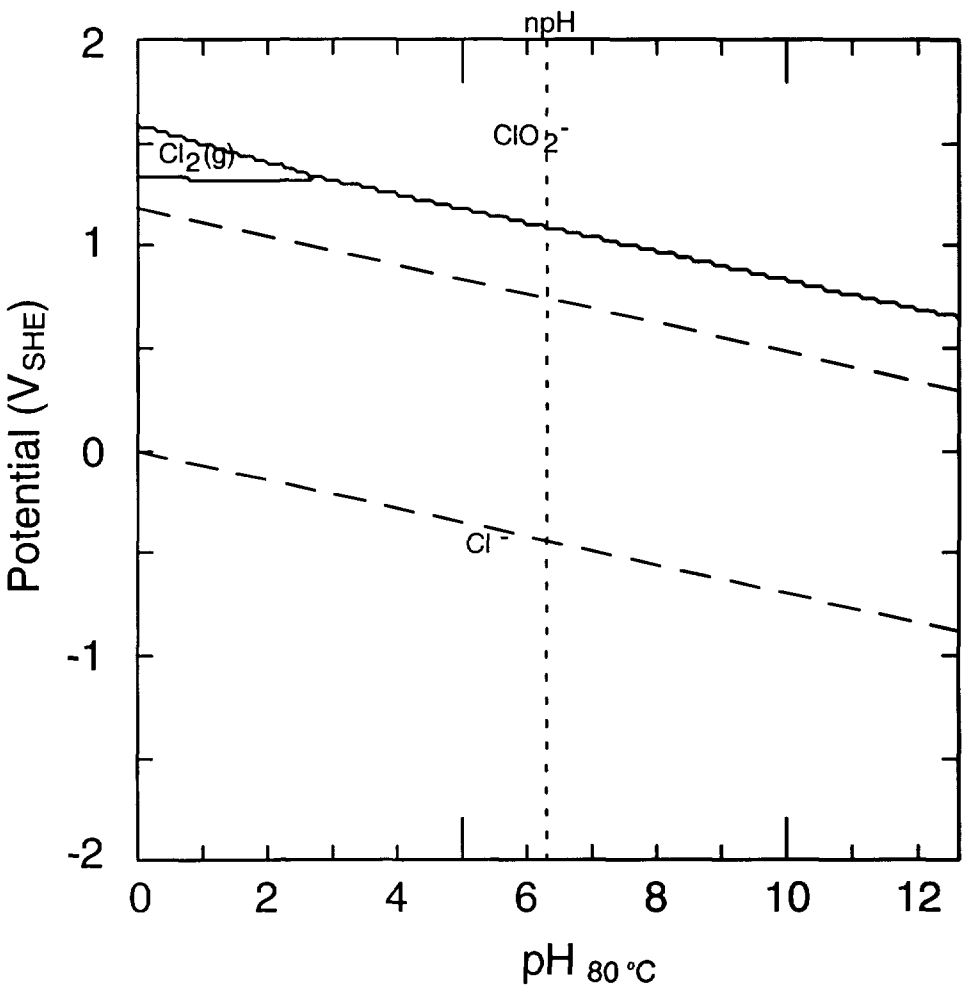


**Figure 1D**
Pourbaix diagram for chlorine at 80 °C and $[Cl(aq)]_{tot}$ = 0.2 molal.

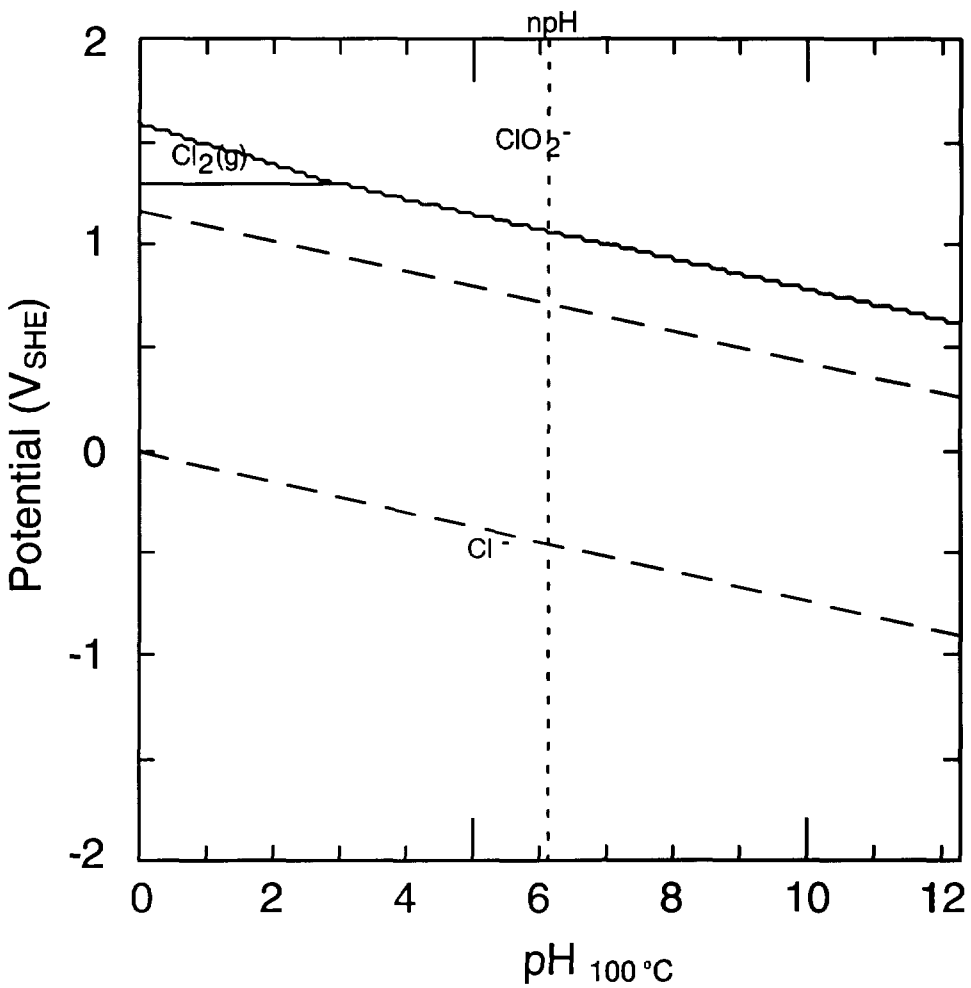


**Figure 1E**
Pourbaix diagram for chlorine at 100 °C and $[Cl(aq)]_{tot}$ = 0.2 molal.

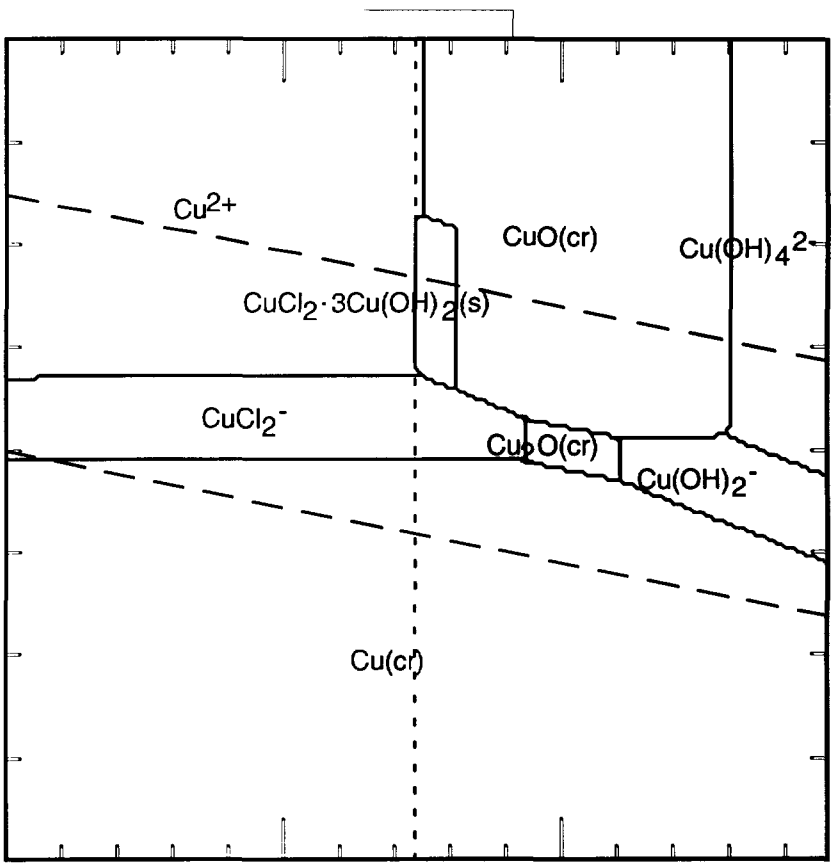
Cu2+
CuO(cr)
Cu(OH)42-
CuCl2·3Cu(OH)2(s)
CuCl2-
Cu2O(cr)
Cu(OH)2-
Cu(cr)

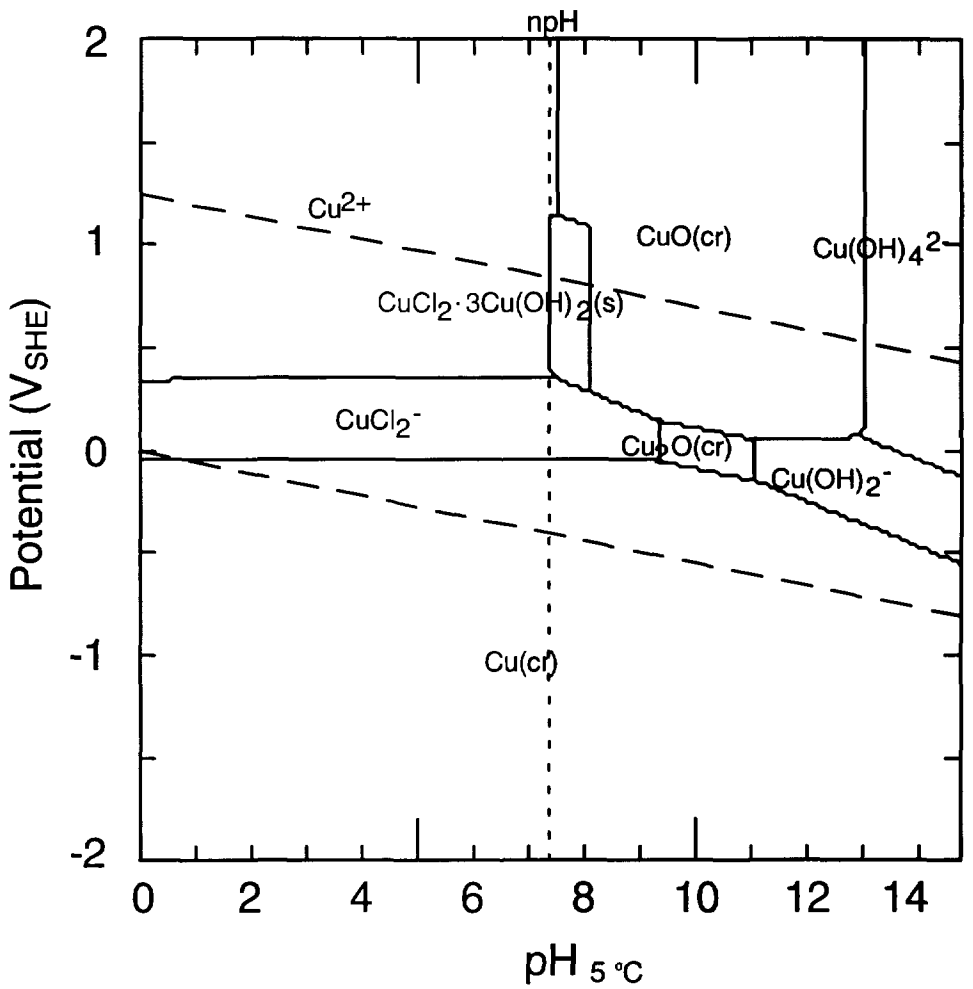


**Figure 2A**
Pourbaix diagram for copper species in the copper-chlorine-water system at 5 °C and $[Cu(aq)]_{tot} = 10^{-6}$ molal and $[Cl(aq)]_{tot} = 0.2$ molal.

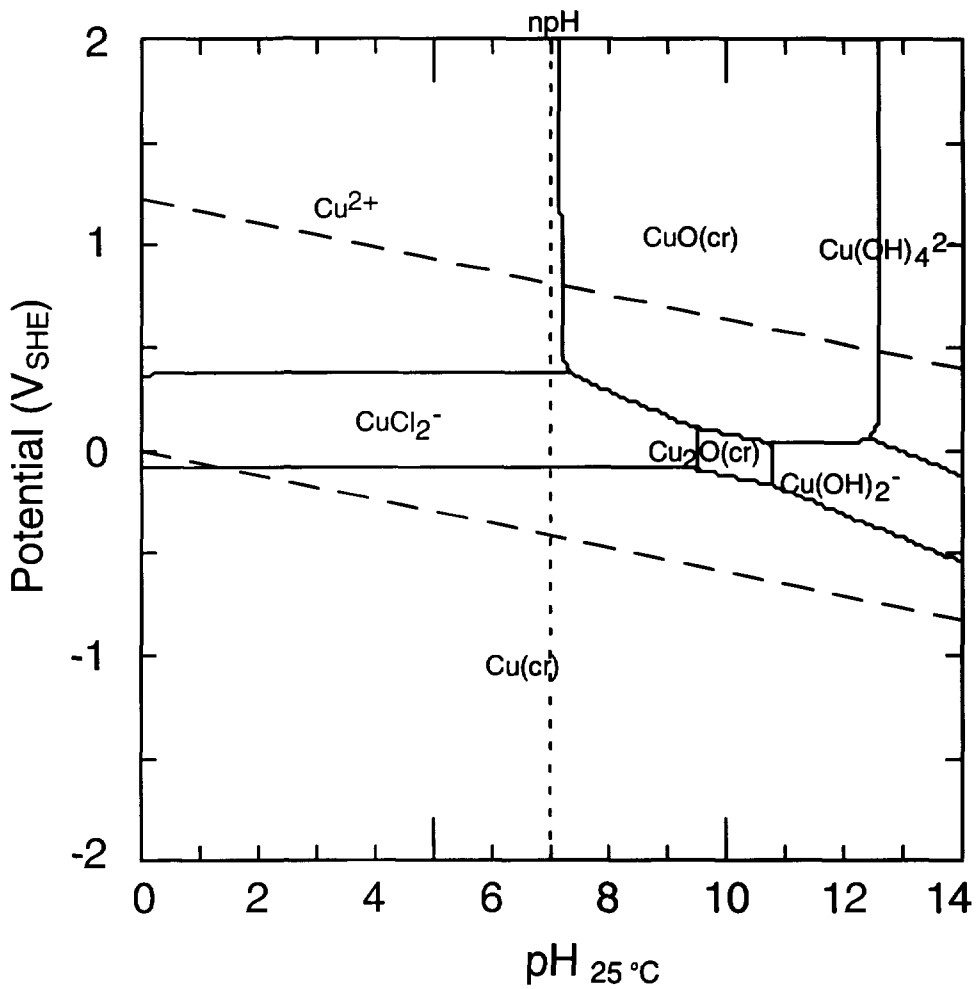


**Figure 2B**
Pourbaix diagram for copper species in the copper-chlorine-water system at 25 °C and $[Cu(aq)]_{tot} = 10^{-6}$ molal and $[Cl(aq)]_{tot} = 0.2$ molal.

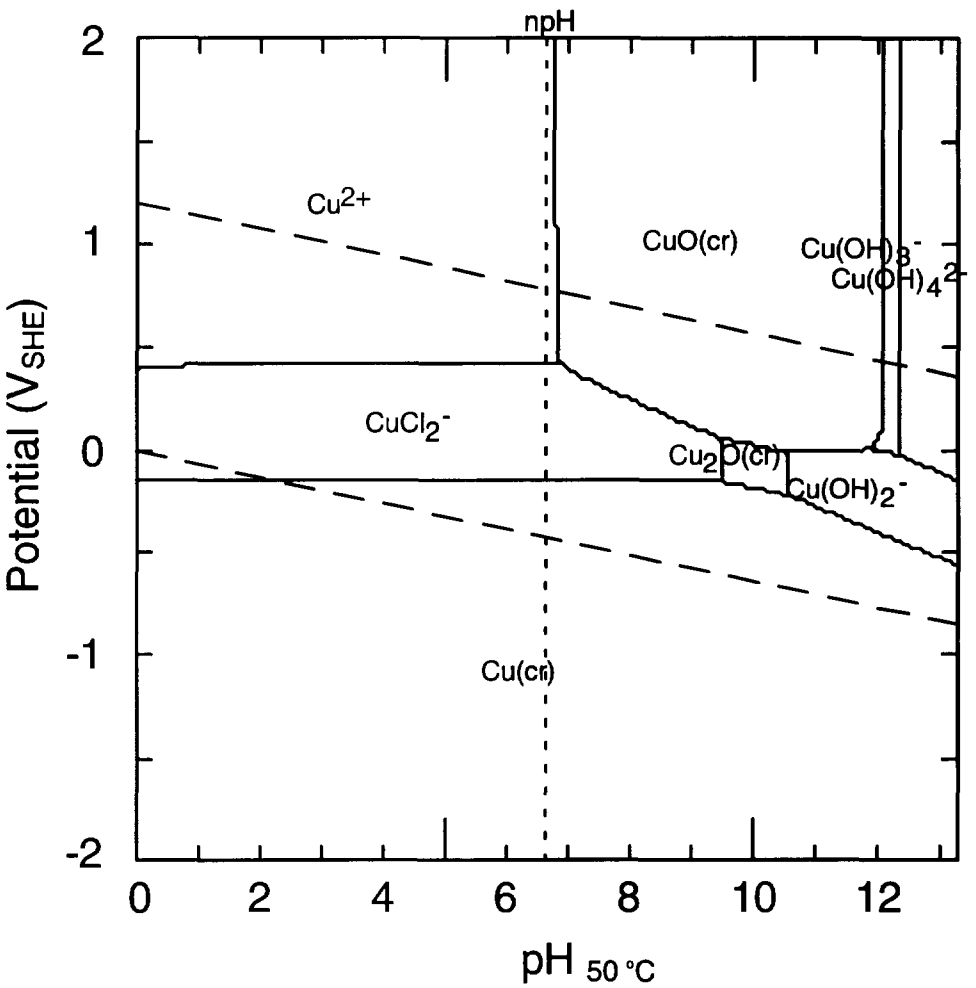


**Figure 2C**
Pourbaix diagram for copper species in the copper-chlorine-water system at 50 °C and $[Cu(aq)]_{tot} = 10^{-6}$ molal and $[Cl(aq)]_{tot} = 0.2$ molal.

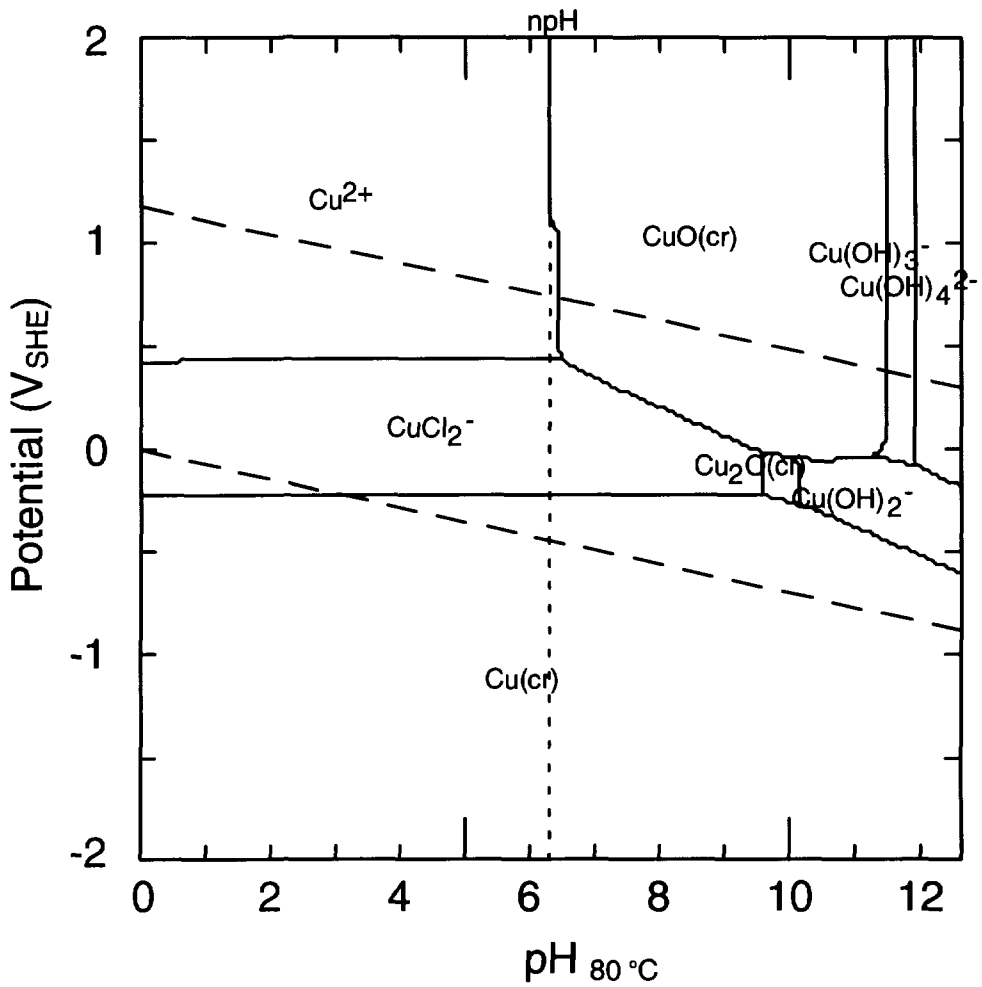


**Figure 2D**
Pourbaix diagram for copper species in the copper-chlorine-water system at 80 °C and $[Cu(aq)]_{tot} = 10^{-6}$ molal and $[Cl(aq)]_{tot} = 0.2$ molal.

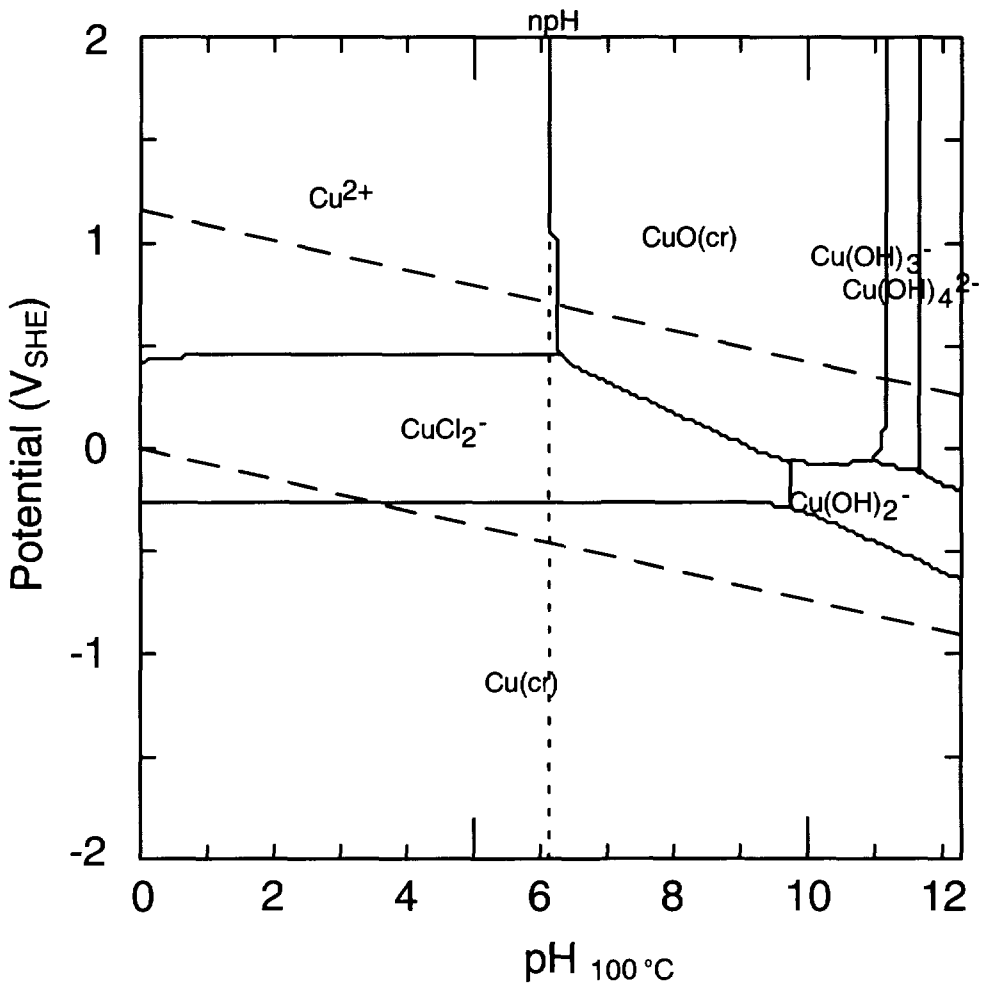


**Figure 2E**
Pourbaix diagram for copper species in the copper-chlorine-water system at 100 °C and $[Cu(aq)]_{tot} = 10^{-6}$ molal and $[Cl(aq)]_{tot} = 0.2$ molal.

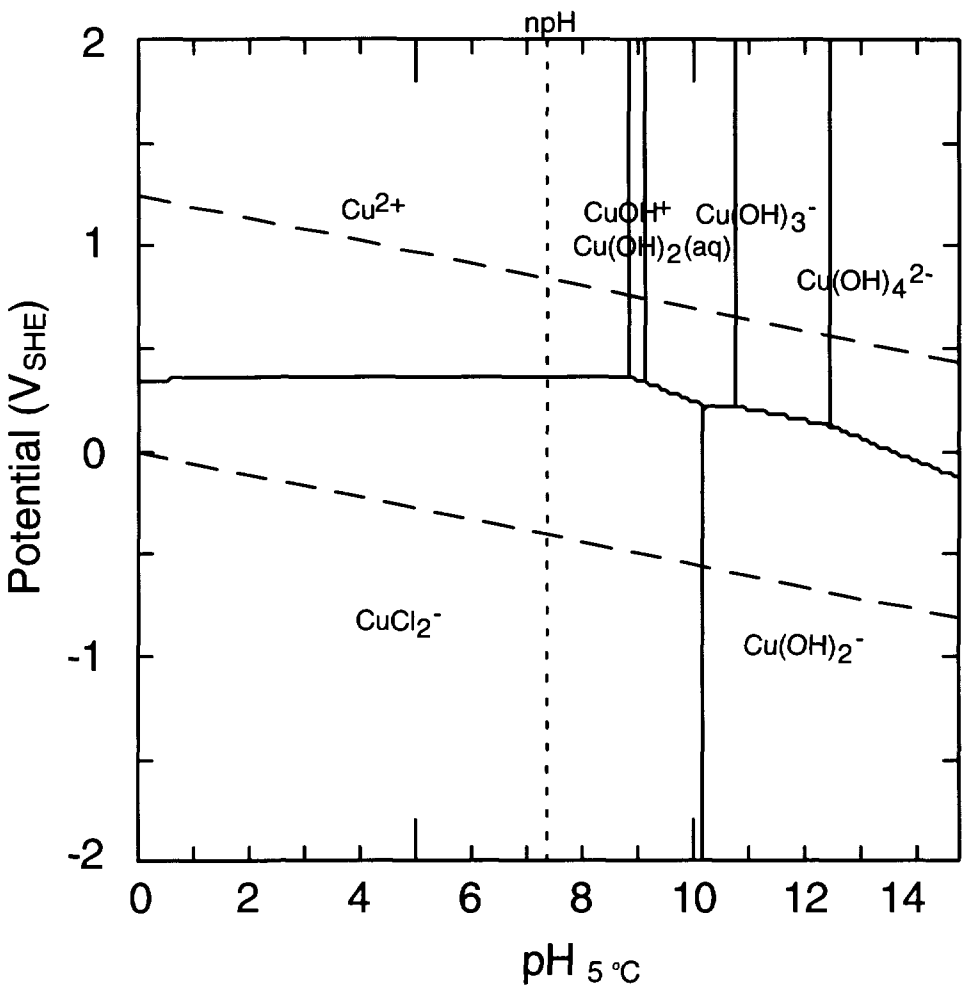


**Figure 3A**
Predominance diagram for dissolved copper species in the copper-chlorine-water system at 5 °C and $[Cu(aq)]_{tot} = 10^{-6}$ molal and $[Cl(aq)]_{tot} = 0.2$ molal.

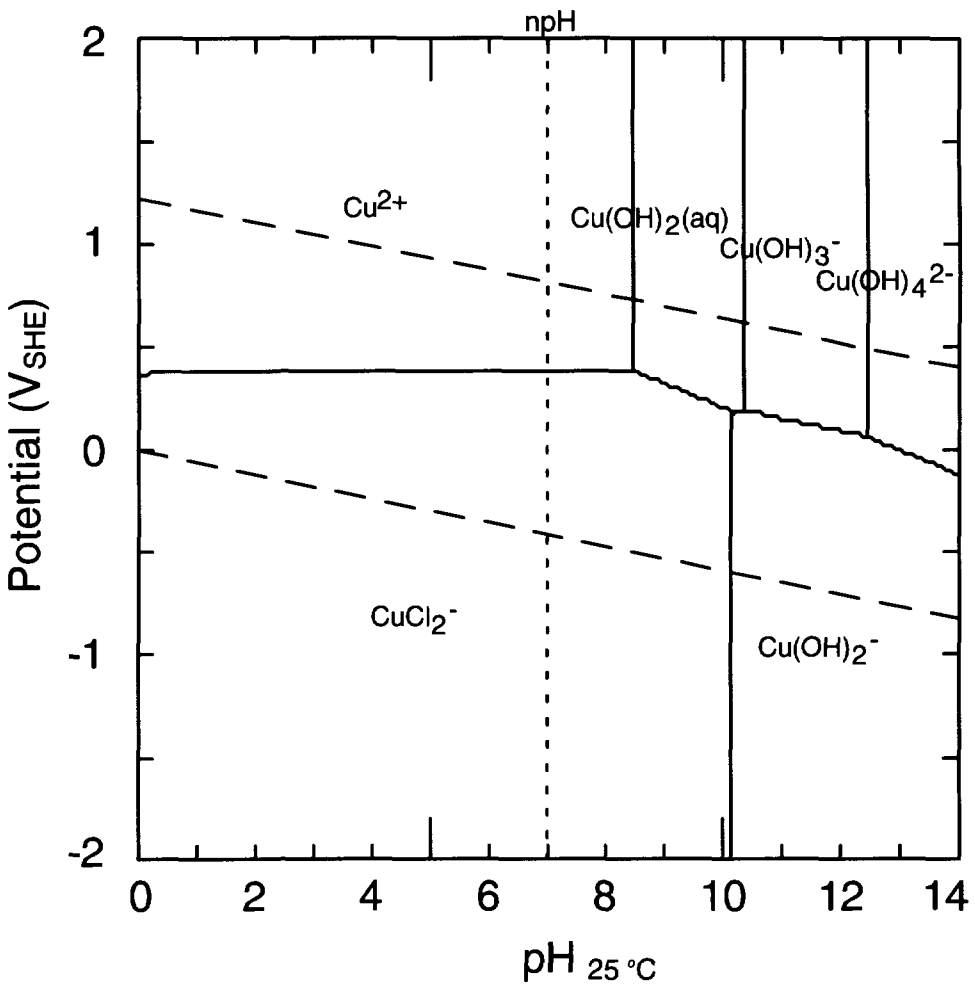


**Figure 3B**
Predominance diagram for dissolved copper species in the copper-chlorine-water system at 25 °C and $[Cu(aq)]_{tot} = 10^{-6}$ molal and $[Cl(aq)]_{tot} = 0.2$ molal.

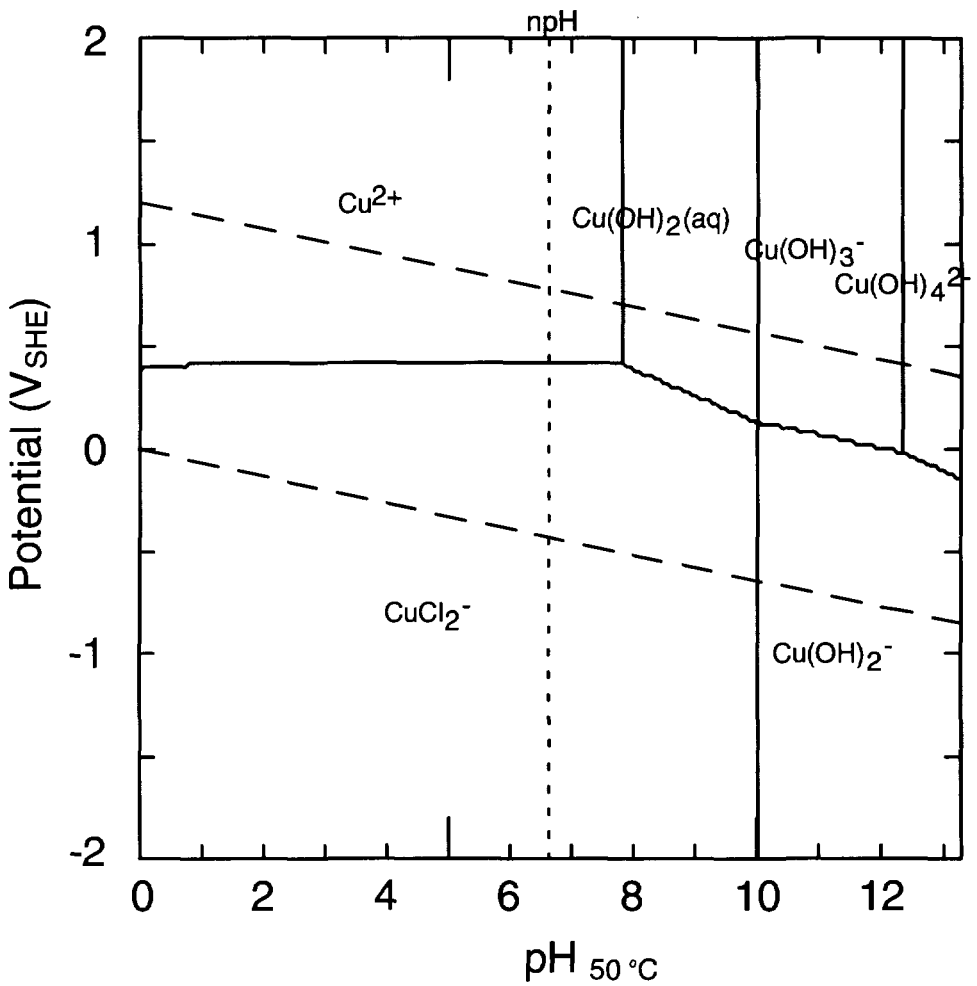


**Figure 3C**
Predominance diagram for dissolved copper species in the copper-chlorine-water system at 50 °C and $[Cu(aq)]_{tot} = 10^{-6}$ molal and $[Cl(aq)]_{tot} = 0.2$ molal.

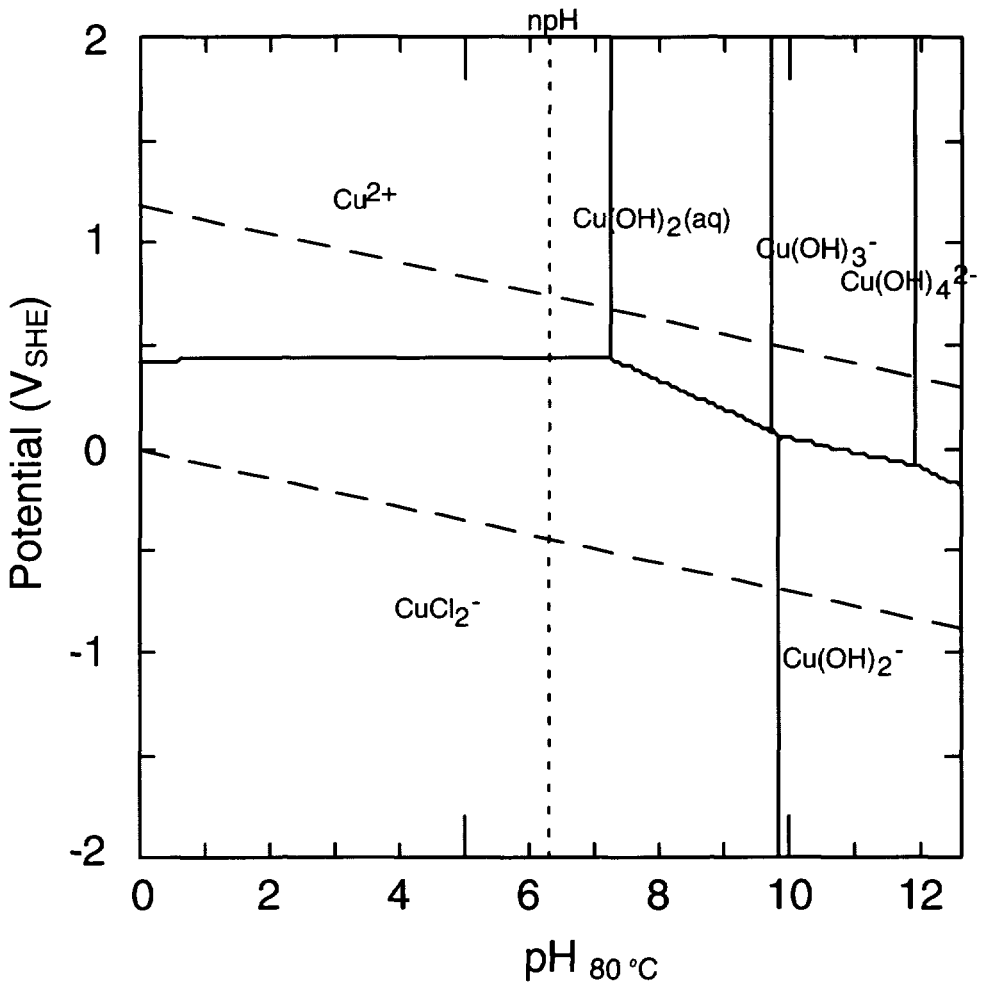


**Figure 3D**
Predominance diagram for dissolved copper species in the copper-chlorine-water system at 80 °C and $[Cu(aq)]_{tot} = 10^{-6}$ molal and $[Cl(aq)]_{tot} = 0.2$ molal.

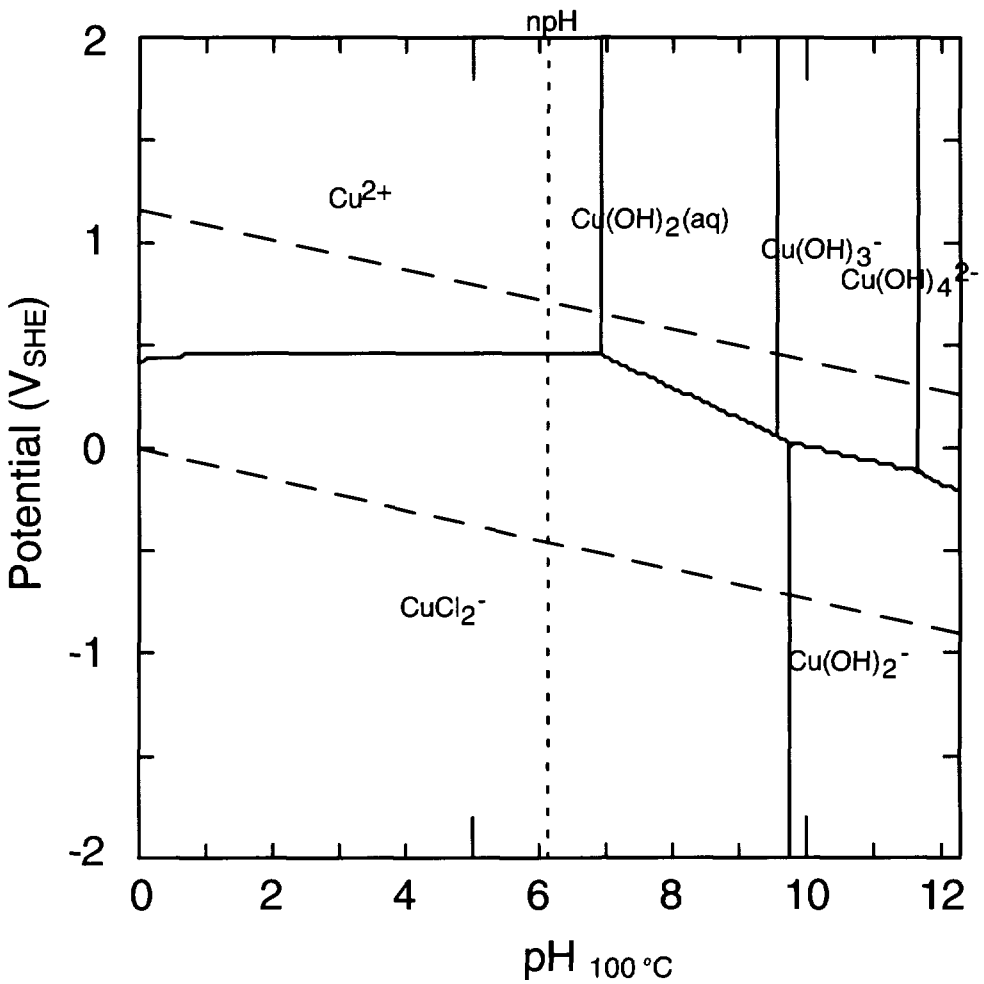


**Figure 3E**
Predominance diagram for dissolved copper species in the copper-chlorine-water system at 100 °C and $[Cu(aq)]_{tot} = 10^{-6}$ molal and $[Cl(aq)]_{tot} = 0.2$ molal.

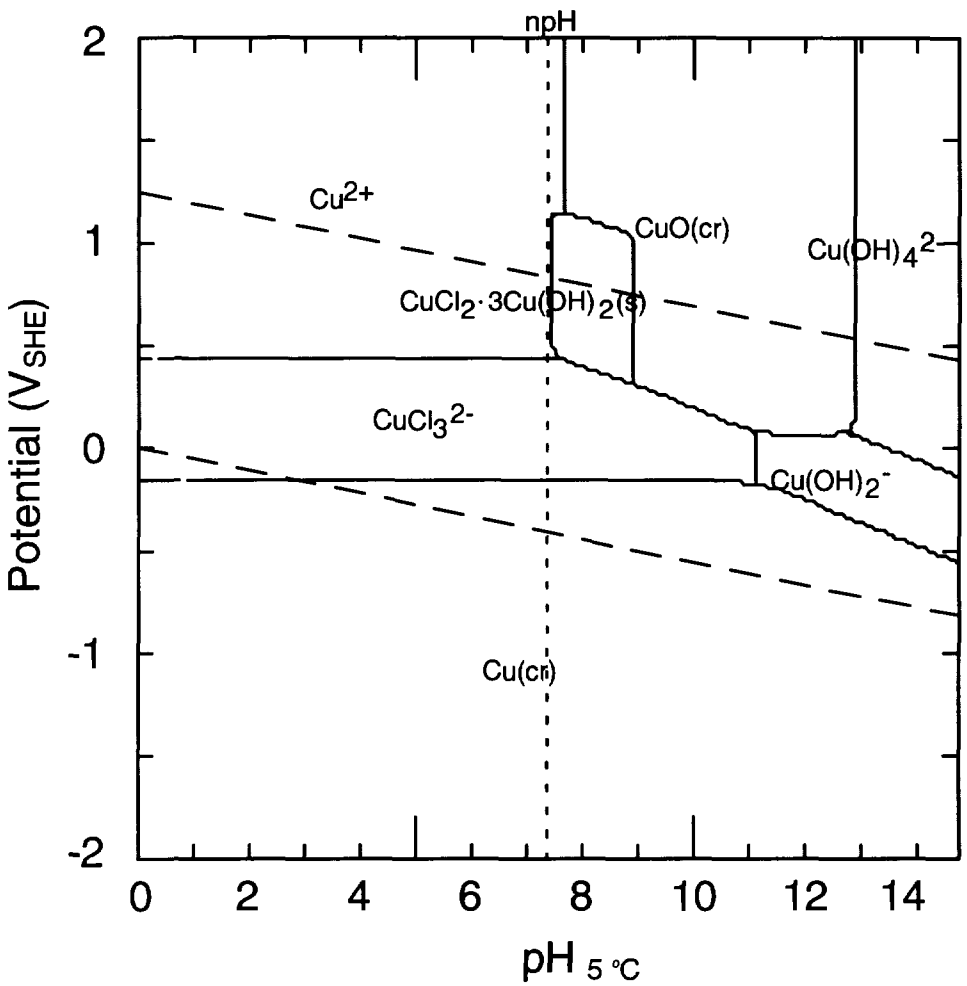


**Figure 4A**
Pourbaix diagram for copper species in the copper-chlorine-water system at 5 °C and $[Cu(aq)]_{tot} = 10^{-6}$ molal $[Cl(aq)]_{tot} = 1.5$ molal.

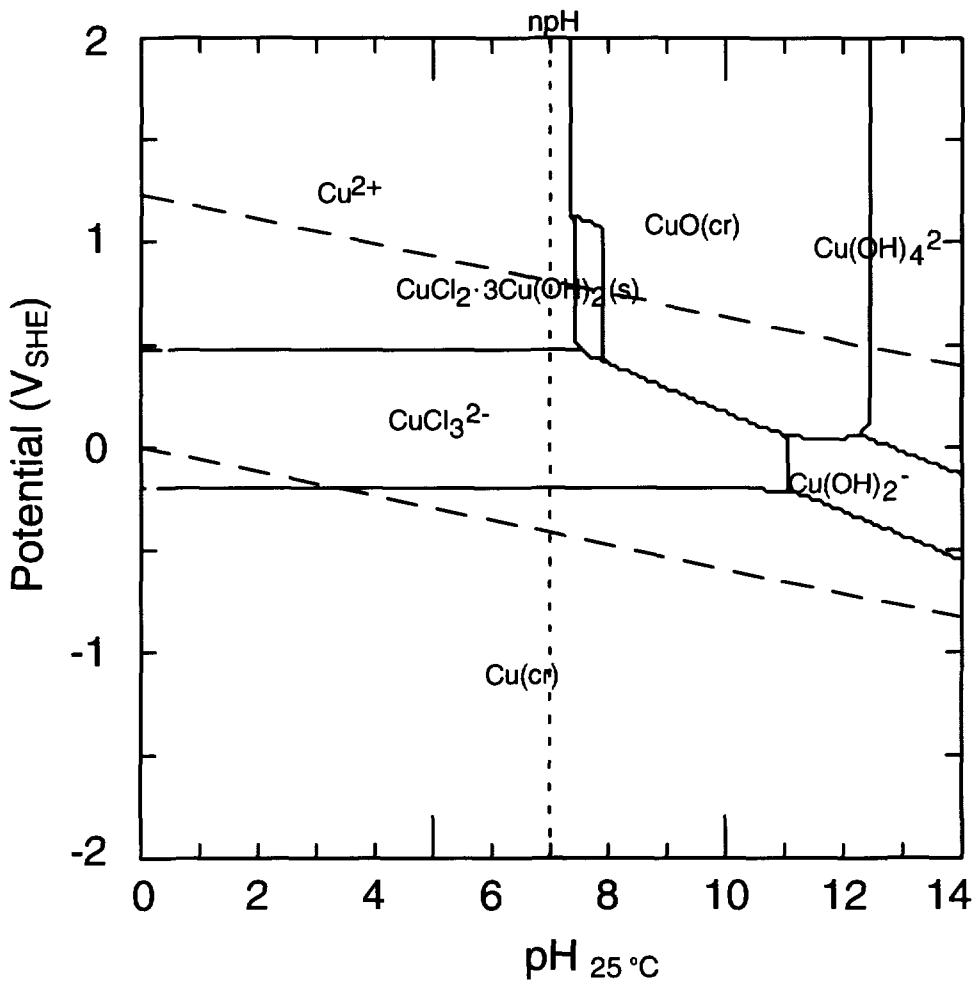


**Figure 4B**
Pourbaix diagram for copper species in the copper-chlorine-water system at 25 °C and $[Cu(aq)]_{tot} = 10^{-6}$ molal and $[Cl(aq)]_{tot} = 1.5$ molal.

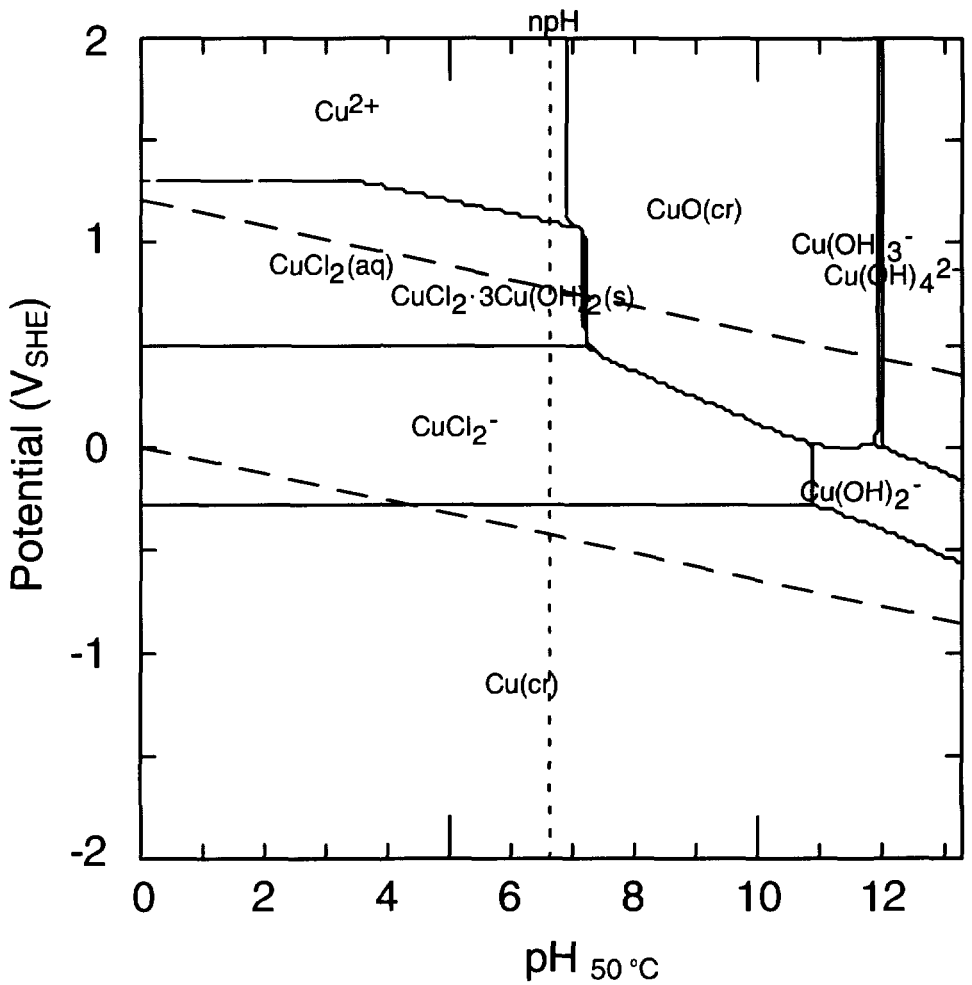


**Figure 4C**
Pourbaix diagram for copper species in the copper-chlorine-water system at 50 °C and $[Cu(aq)]_{tot} = 10^{-6}$ molal and $[Cl(aq)]_{tot} = 1.5$ molal.

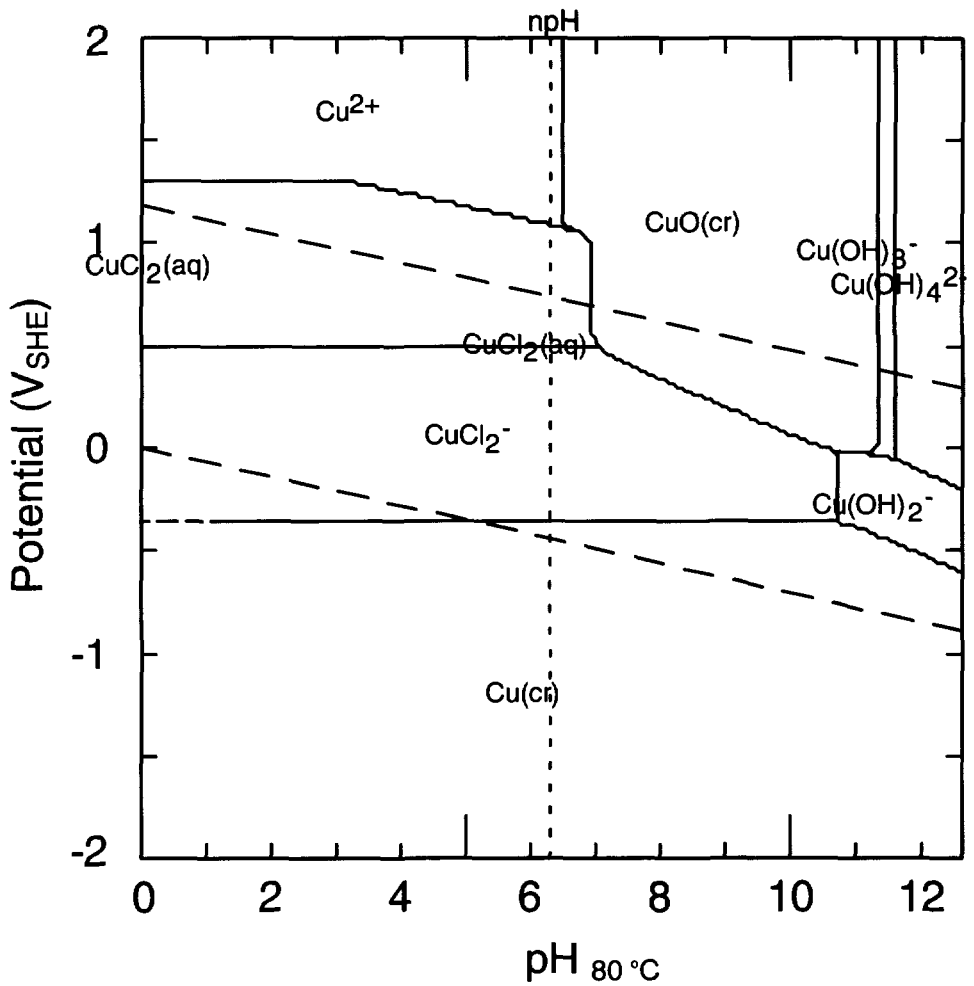


**Figure 4D**
Pourbaix diagram for copper species in the copper-chlorine-water system at 80 °C and $[Cu(aq)]_{tot} = 10^{-6}$ molal and $[Cl(aq)]_{tot} = 1.5$ molal.

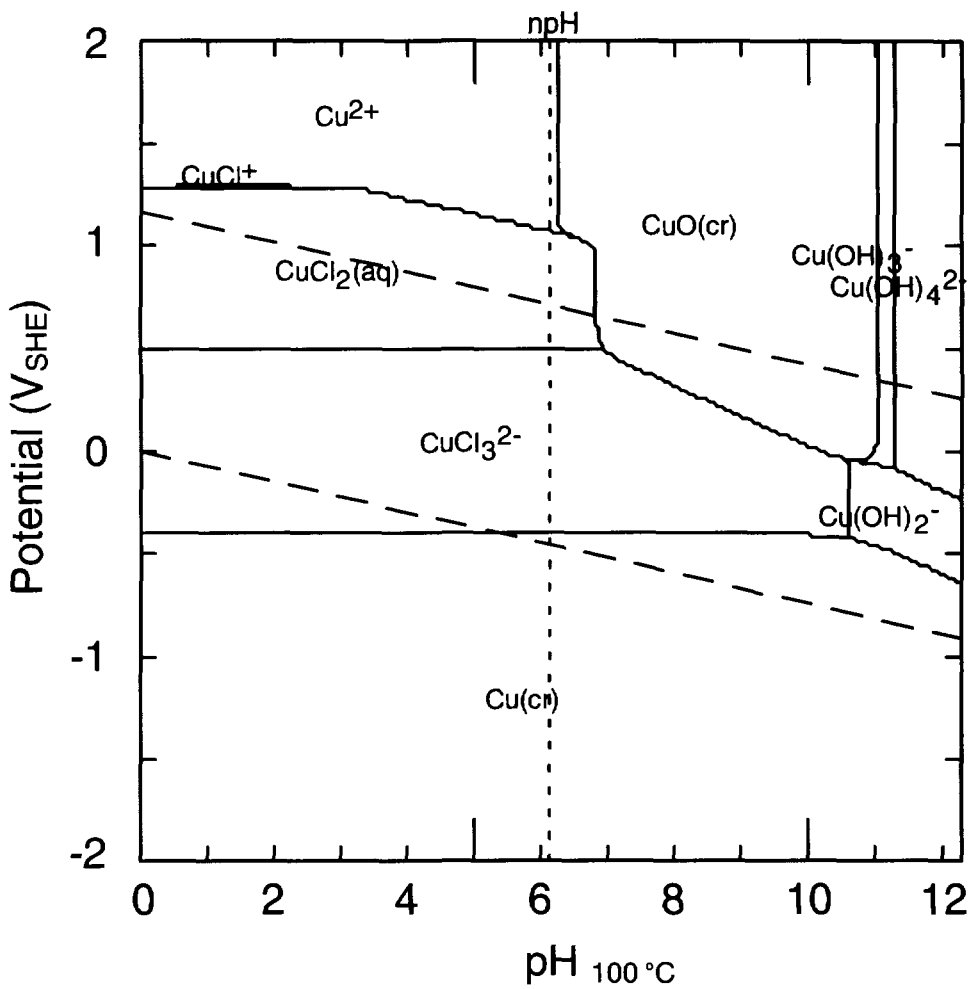


**Figure 4E**
Pourbaix diagram for copper species in the copper-chlorine-water system at 100 °C and $[Cu(aq)]_{tot} = 10^{-6}$ molal and $[Cl(aq)]_{tot} = 1.5$ molal.

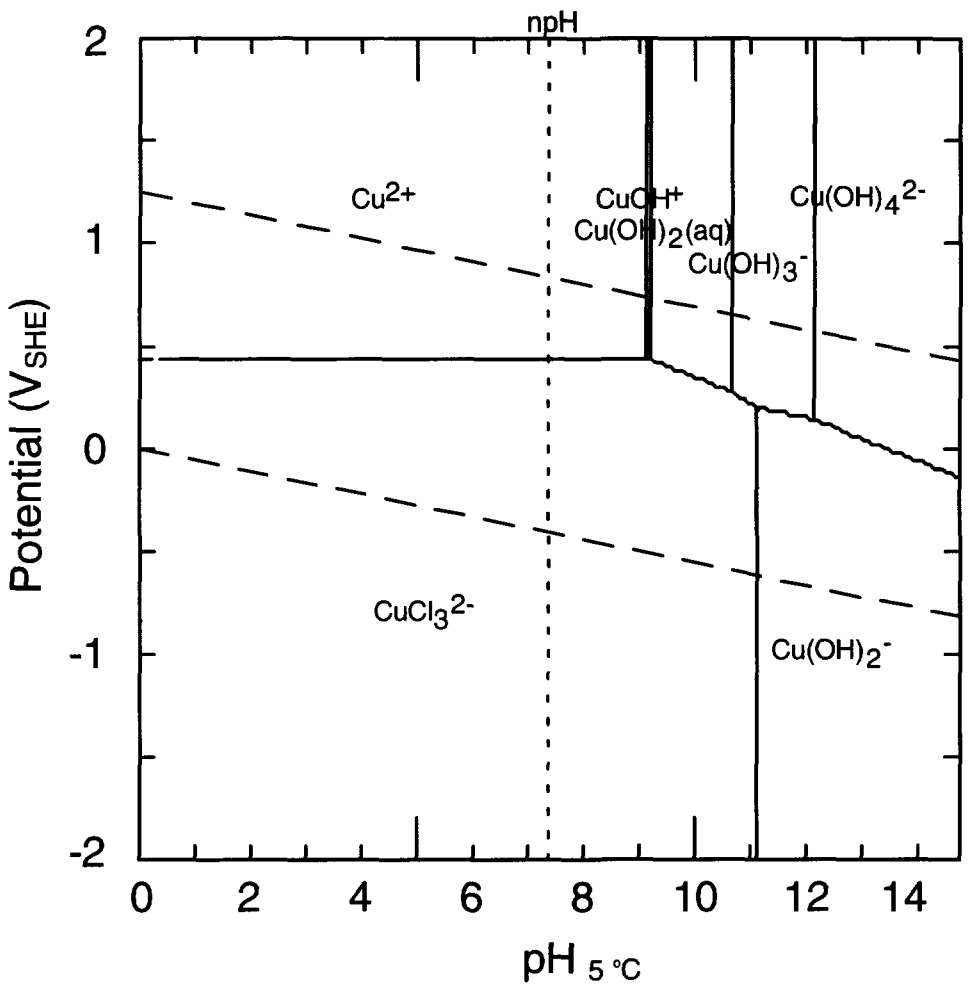


**Figure 5A**
Predominance diagram for dissolved copper species in the copper-chlorine-water system at 5 °C and $[Cu(aq)]_{tot} = 10^{-6}$ molal and $[Cl(aq)]_{tot} = 1.5$ molal.

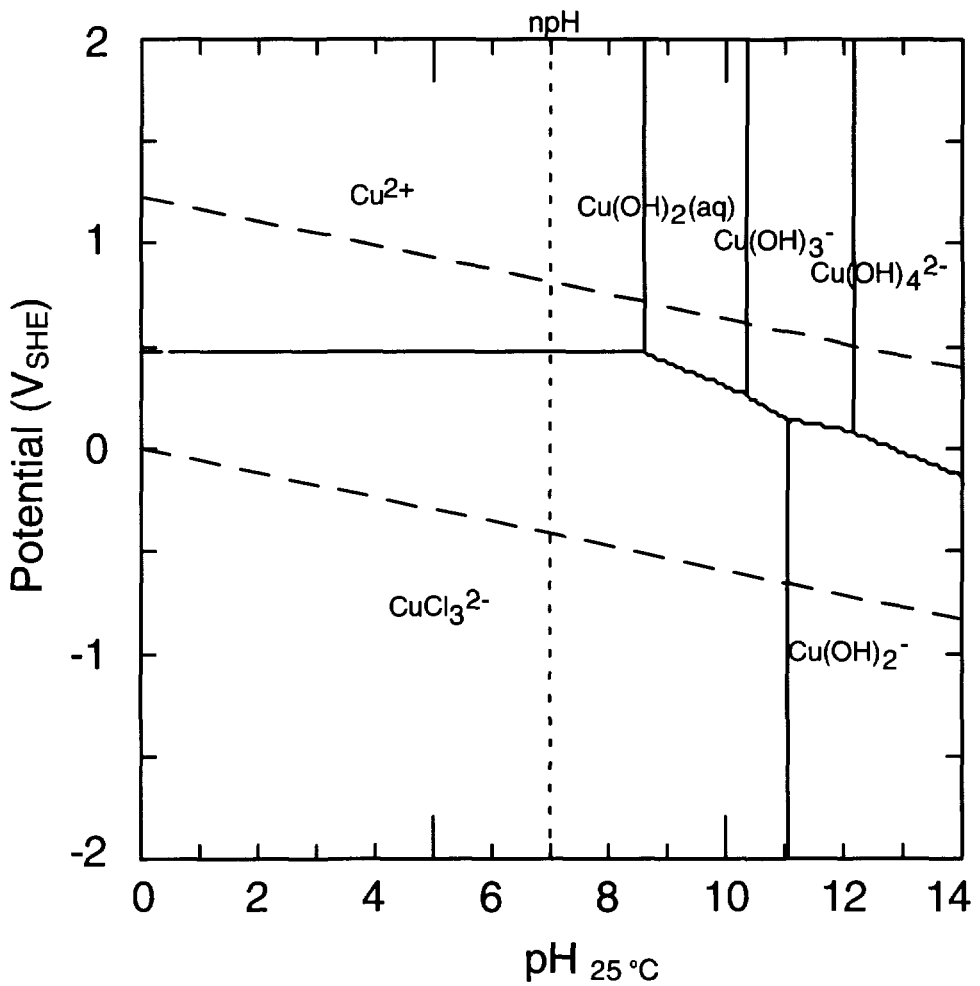


**Figure 5B**
Predominance diagram for dissolved copper species in the copper-chlorine-water system at 25 °C and $[Cu(aq)]_{tot} = 10^{-6}$ molal and $[Cl(aq)]_{tot} = 1.5$ molal.

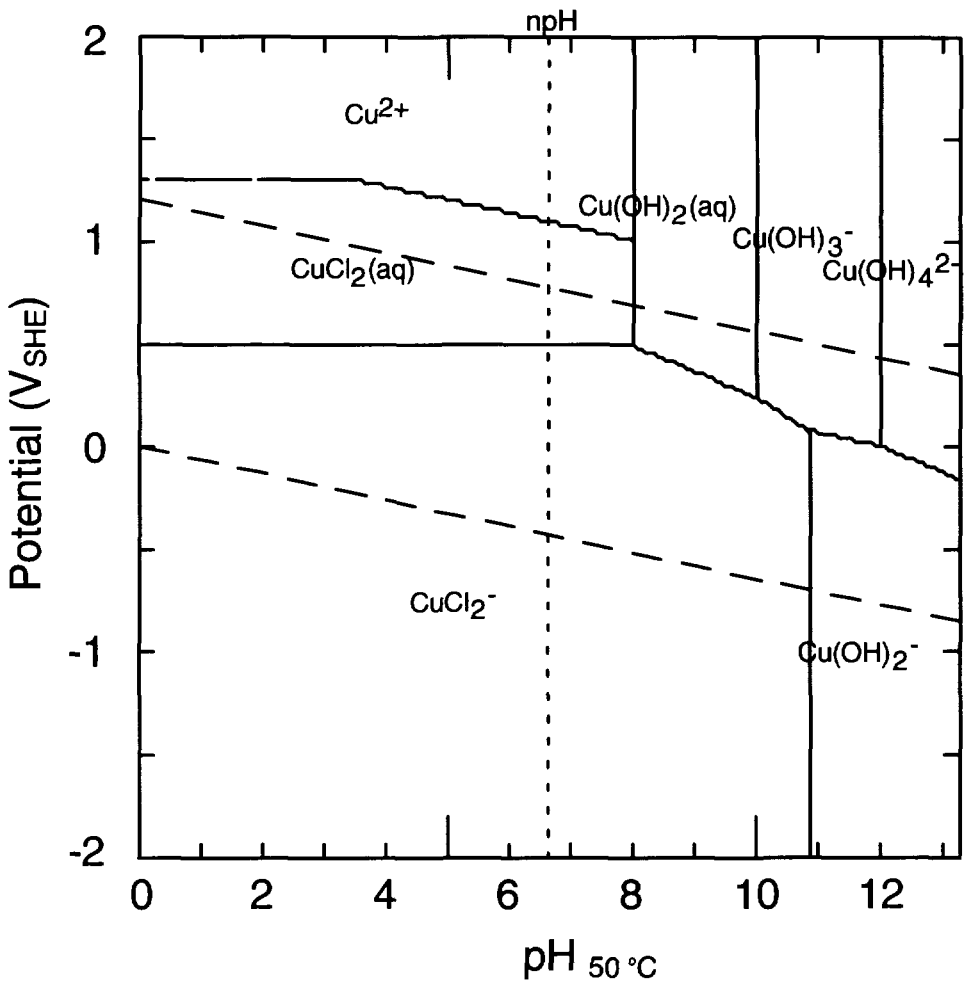


**Figure 5C**
Predominance diagram for dissolved copper species in the copper-chlorine-water system at 50 °C and $[Cu(aq)]_{tot} = 10^{-6}$ molal and $[Cl(aq)]_{tot} = 1.5$ molal.

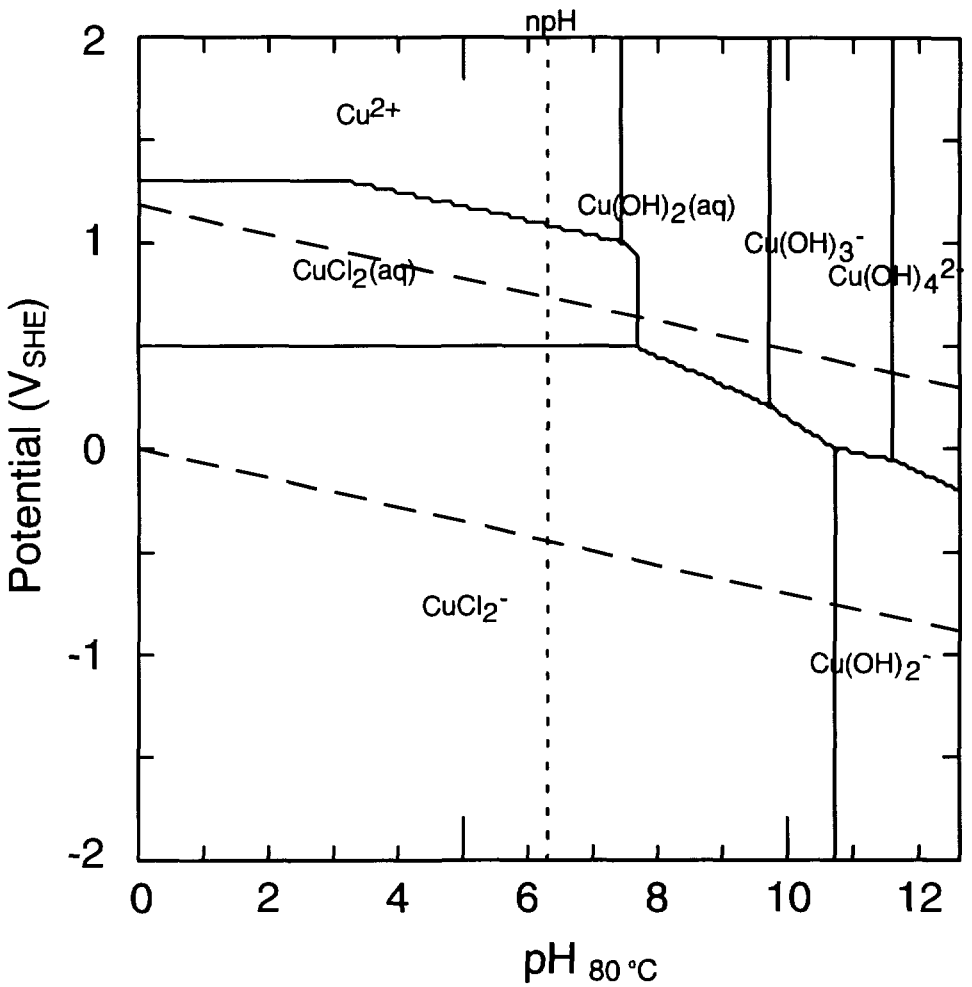


**Figure 5D**
Predominance diagram for dissolved copper species in the copper-chlorine-water system at 80 °C and $[Cu(aq)]_{tot} = 10^{-6}$ molal and $[Cl(aq)]_{tot} = 1.5$ molal.

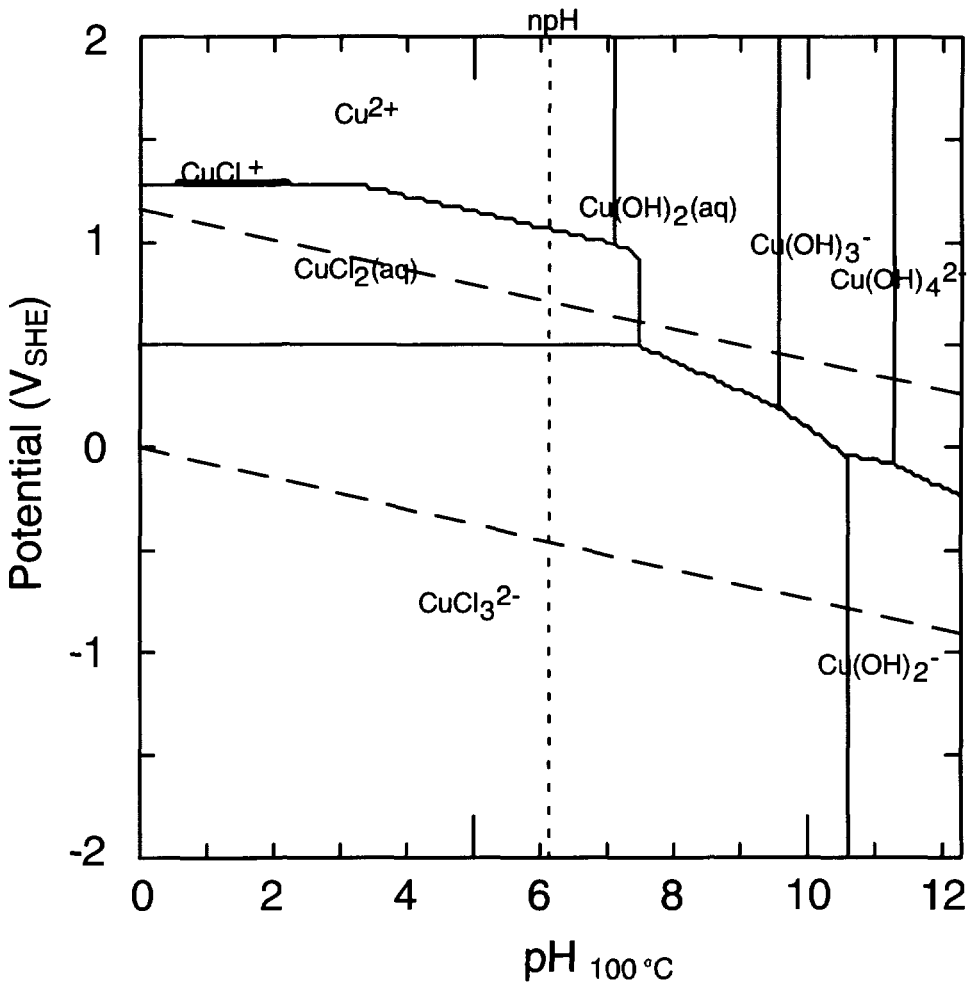


**Figure 5E**
Predominance diagram for dissolved copper species in the copper-chlorine-water system at 100 °C and $[Cu(aq)]_{tot} = 10^{-6}$ molal and $[Cl(aq)]_{tot} = 1.5$ molal.

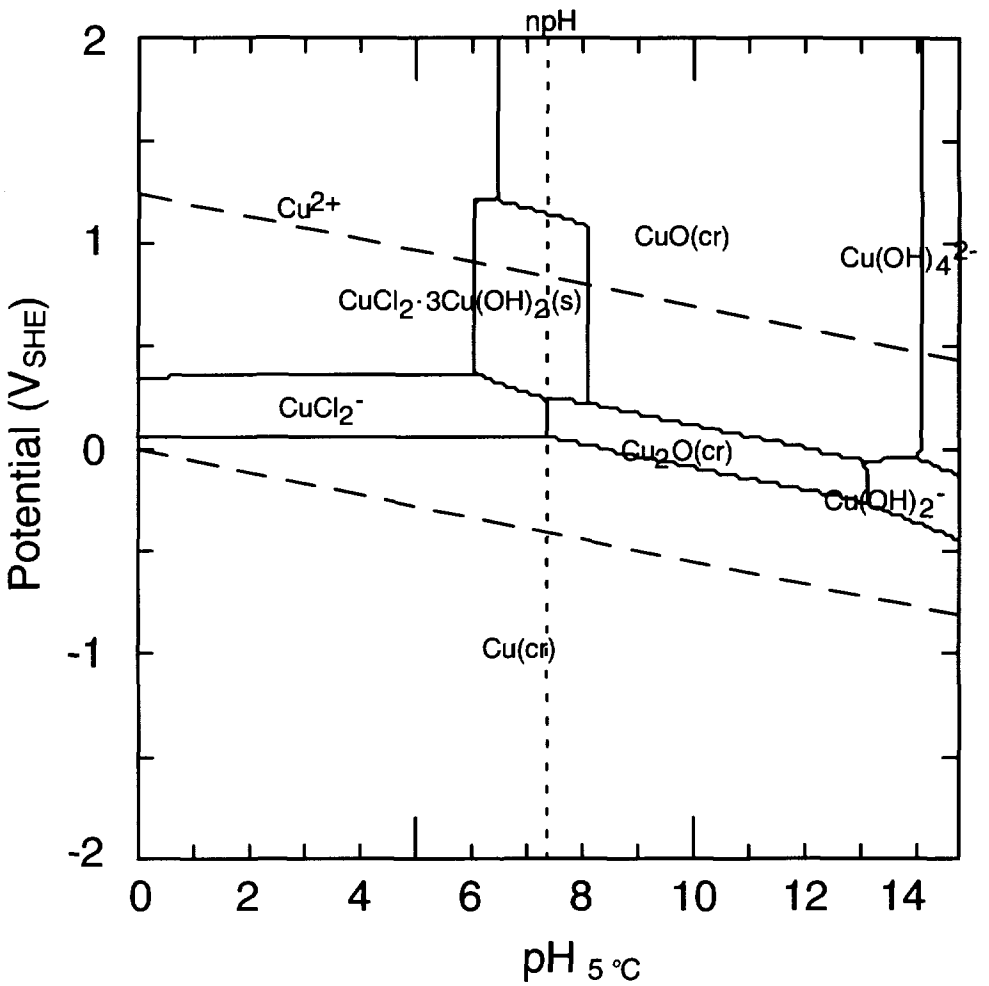


**Figure 6A**
Pourbaix diagram for copper species in the copper-chlorine-water system at 5 °C and $[Cu(aq)]_{tot} = 10^{-4}$ molal and $[Cl(aq)]_{tot} = 0.2$ molal.

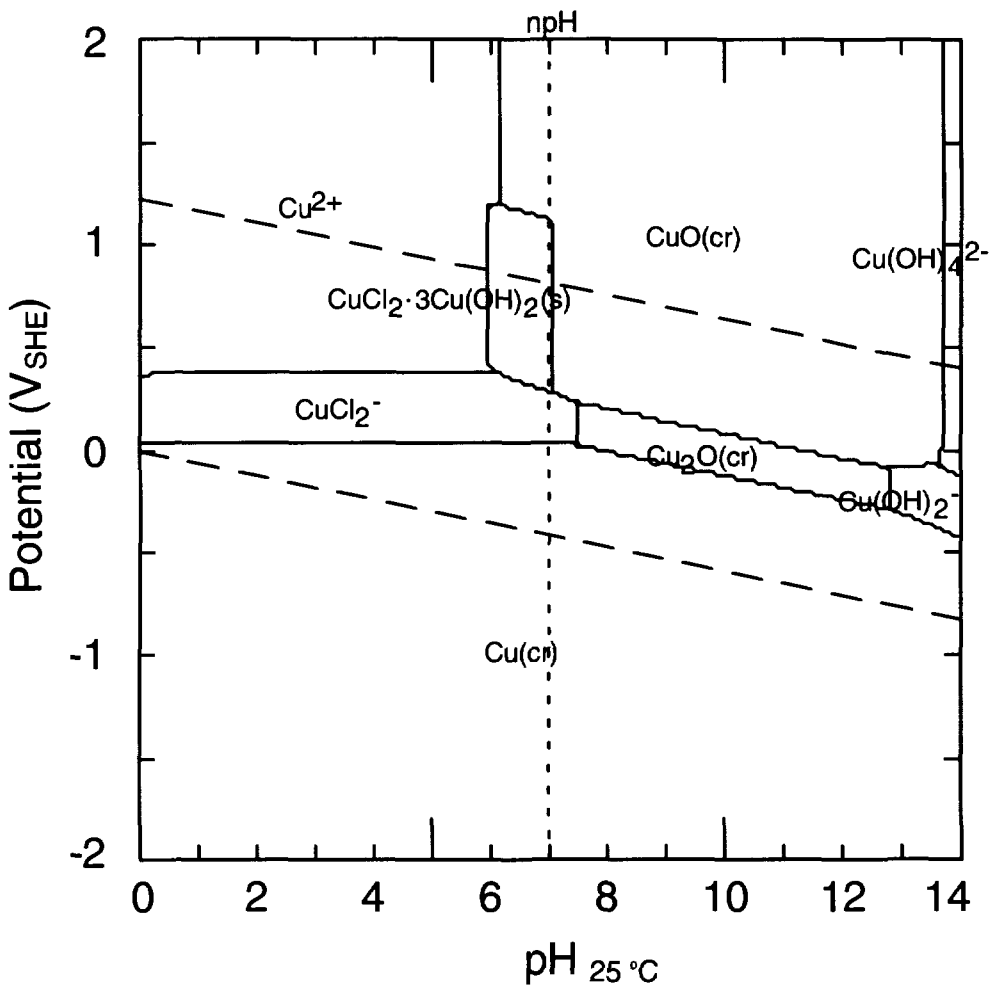


**Figure 6B**
Pourbaix diagram for copper species in the copper-chlorine-water system at 25 °C and $[Cu(aq)]_{tot} = 10^{-4}$ molal and $[Cl(aq)]_{tot} = 0.2$ molal.

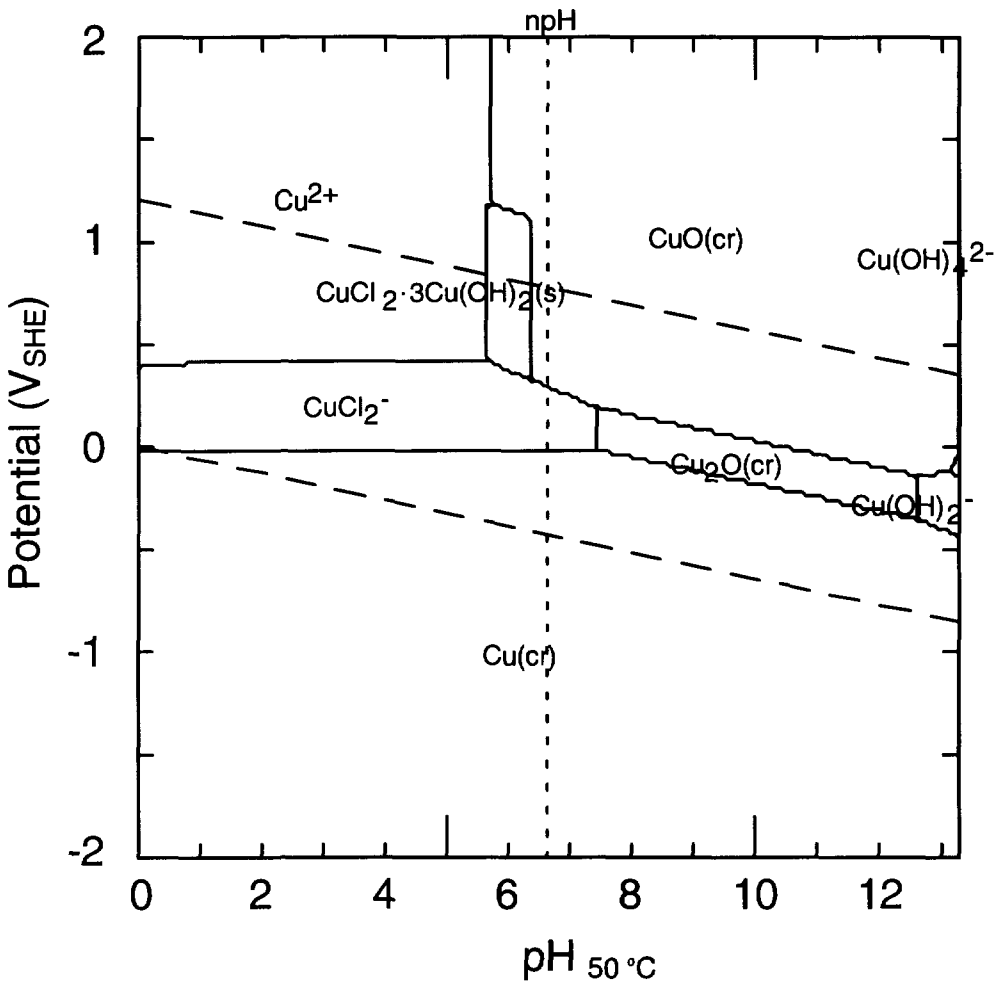


**Figure 6C**
Pourbaix diagram for copper species in the copper-chlorine-water system at 50 °C and $[Cu(aq)]_{tot} = 10^{-4}$ molal and $[Cl(aq)]_{tot} = 0.2$ molal.

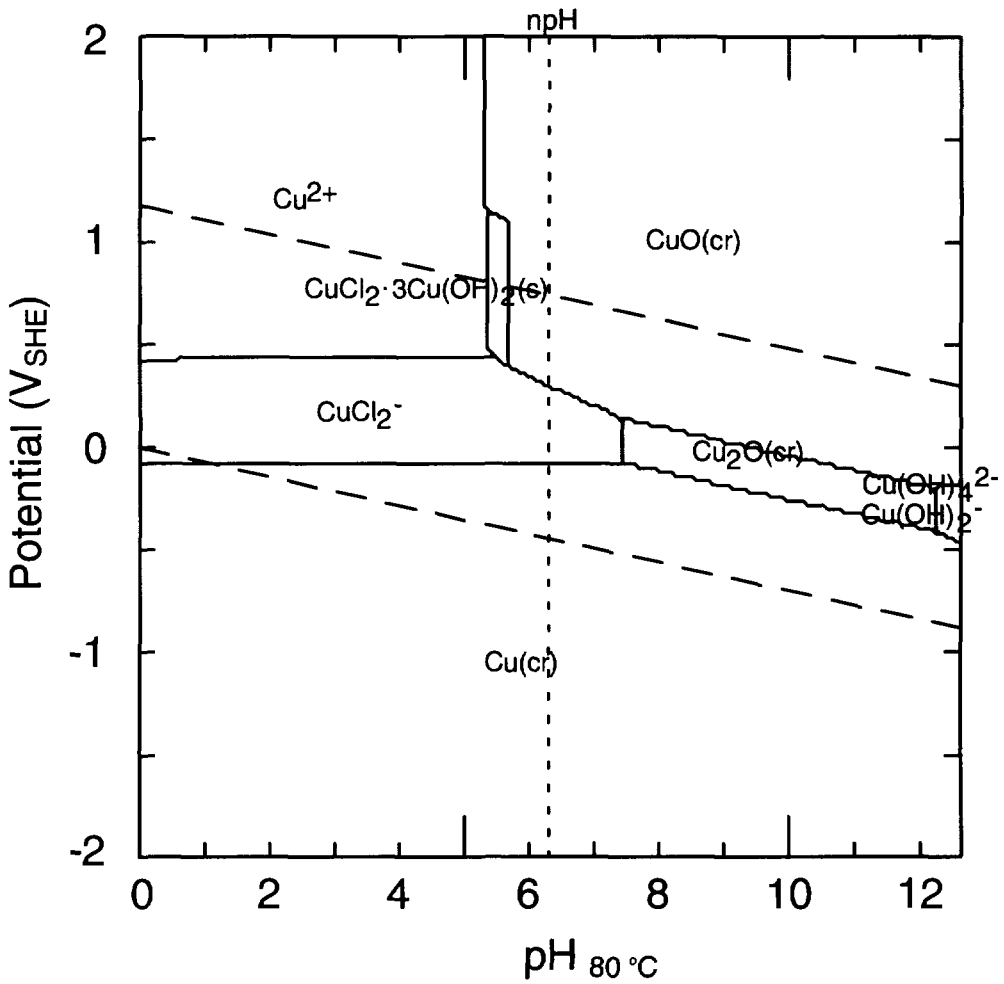


**Figure 6D**
Pourbaix diagram for copper species in the copper-chlorine-water system at 80 °C and $[Cu(aq)]_{tot} = 10^{-4}$ molal and $[Cl(aq)]_{tot} = 0.2$ molal.

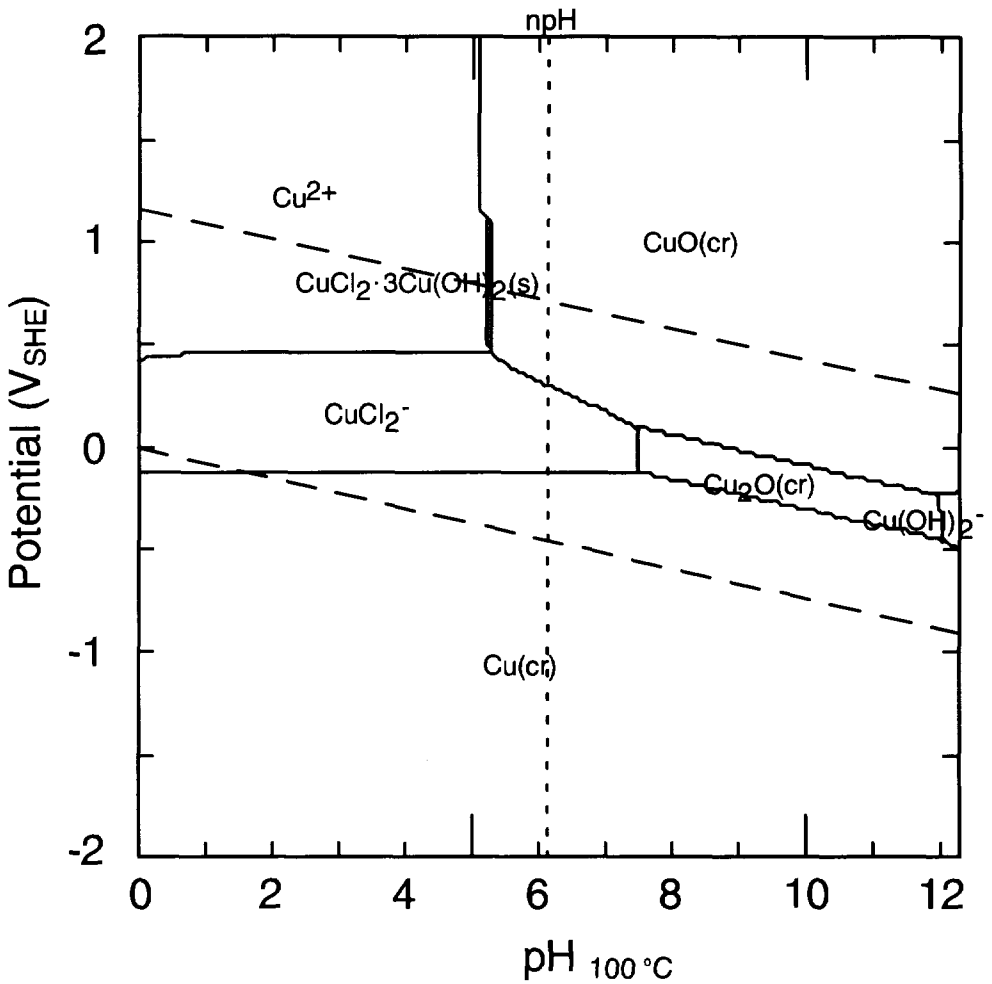


**Figure 6E**
Pourbaix diagram for copper species in the copper-chlorine-water system at 100 °C and $[Cu(aq)]_{tot} = 10^{-4}$ molal and $[Cl(aq)]_{tot} = 0.2$ molal.

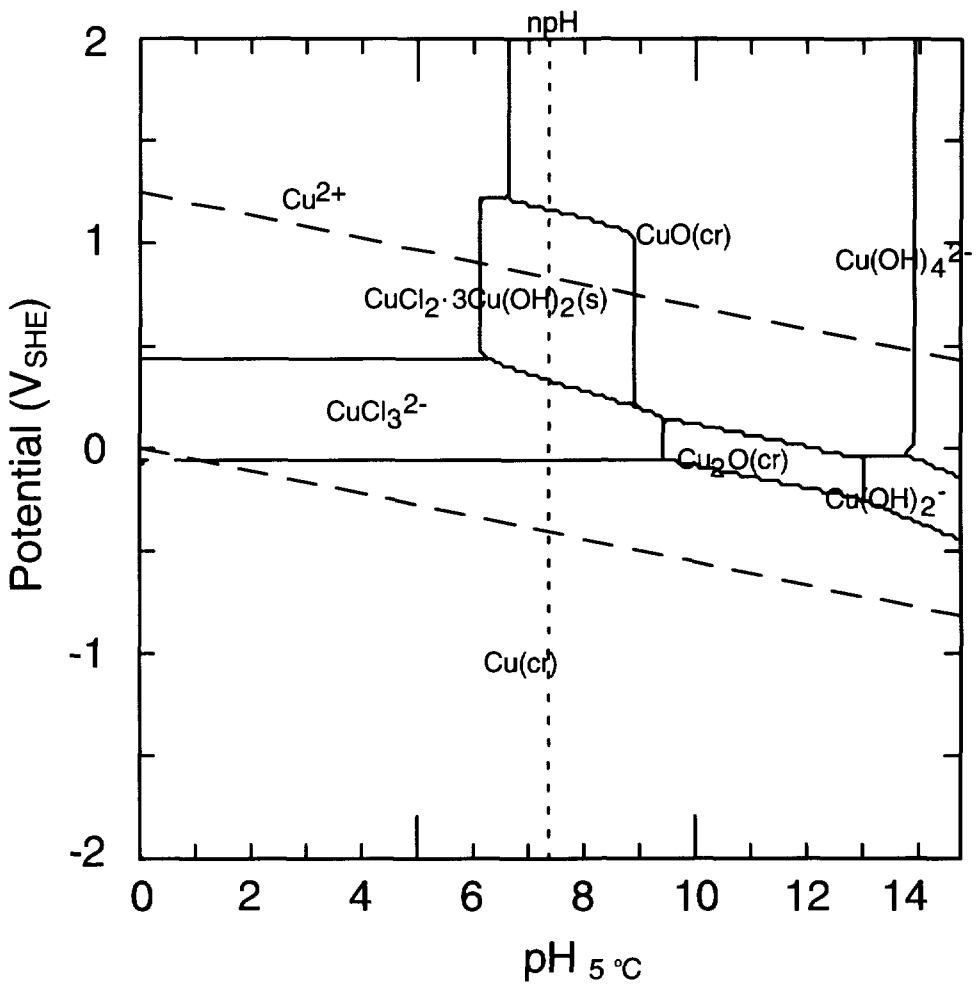


**Figure 7A**
Pourbaix diagram for copper species in the copper-chlorine-water system at 5 °C and $[Cu(aq)]_{tot} = 10^{-4}$ molal and $[Cl(aq)]_{tot} = 1.5$ molal.

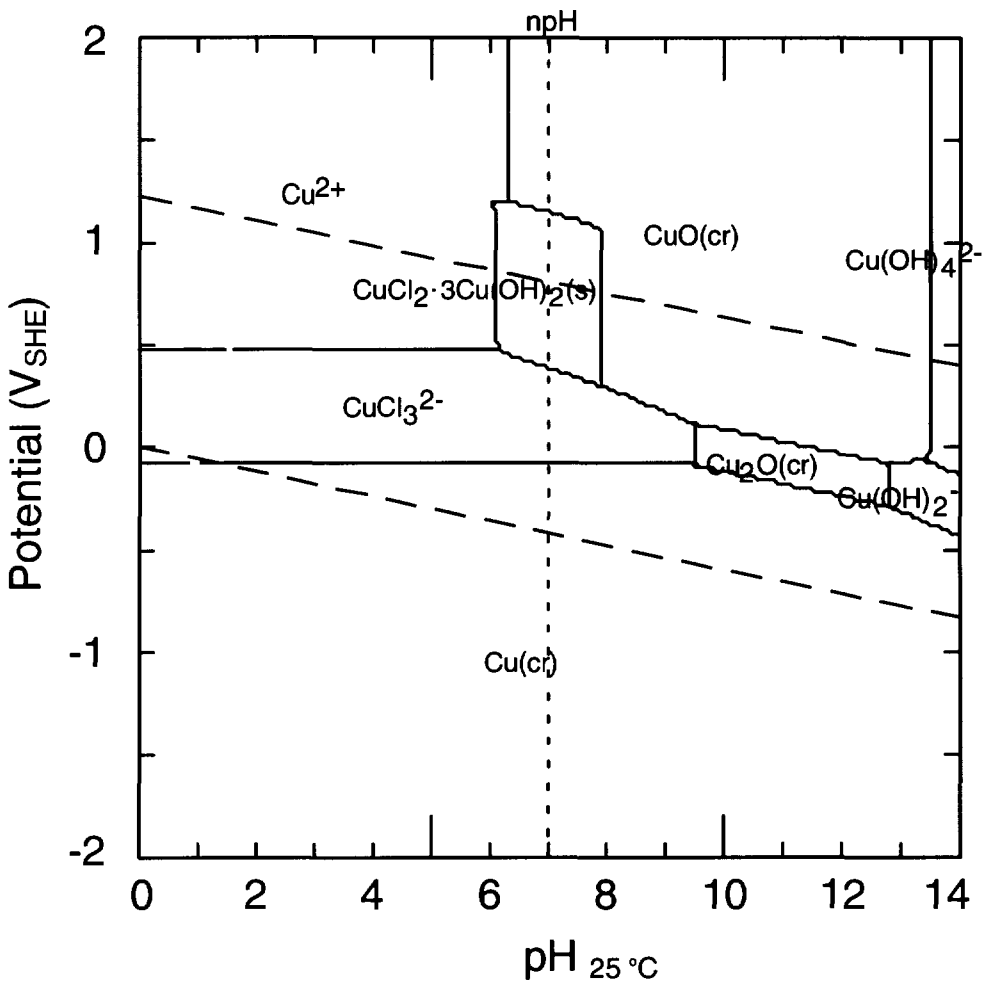


**Figure 7B**
Pourbaix diagram for copper species in the copper-chlorine-water system at 25 °C and $[Cu(aq)]_{tot} = 10^{-4}$ molal and $[Cl(aq)]_{tot} = 1.5$ molal.

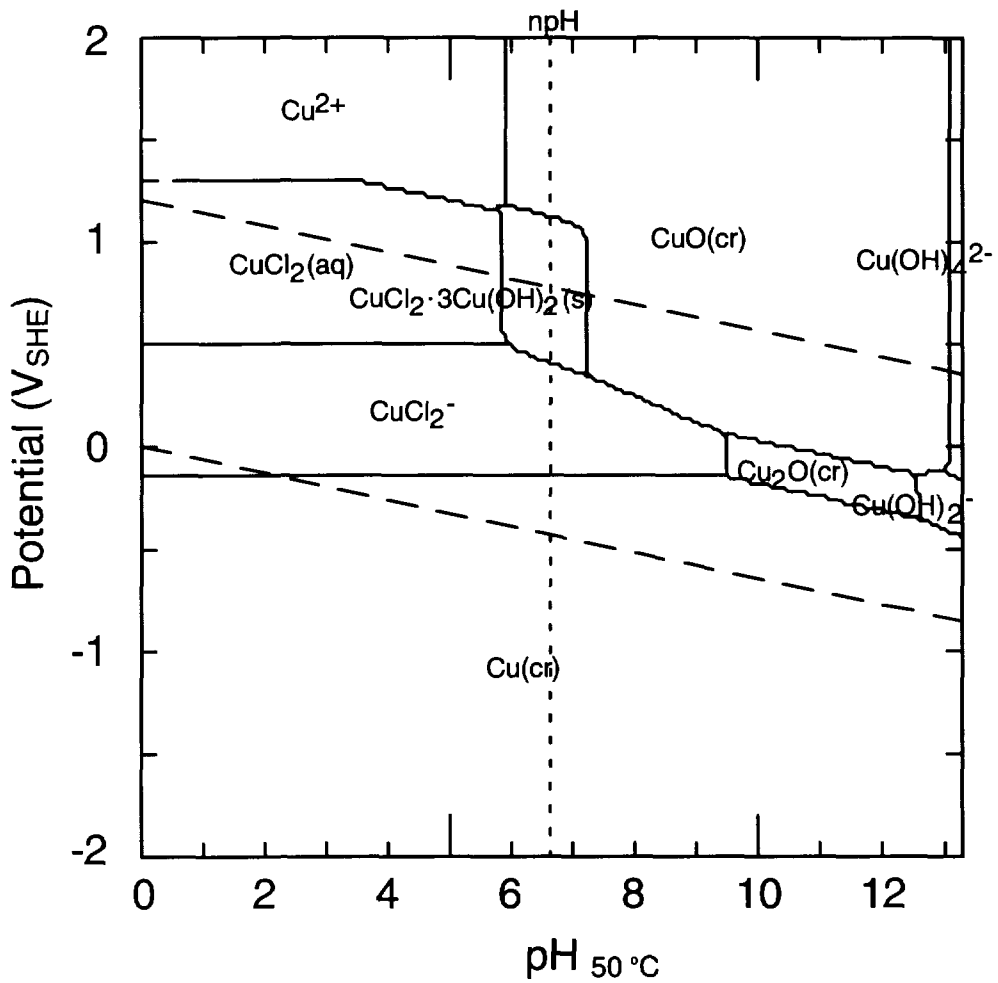


**Figure 7C**
Pourbaix diagram for copper species in the copper-chlorine-water system at 50 °C and $[Cu(aq)]_{tot} = 10^{-4}$ molal and $[Cl(aq)]_{tot} = 1.5$ molal.

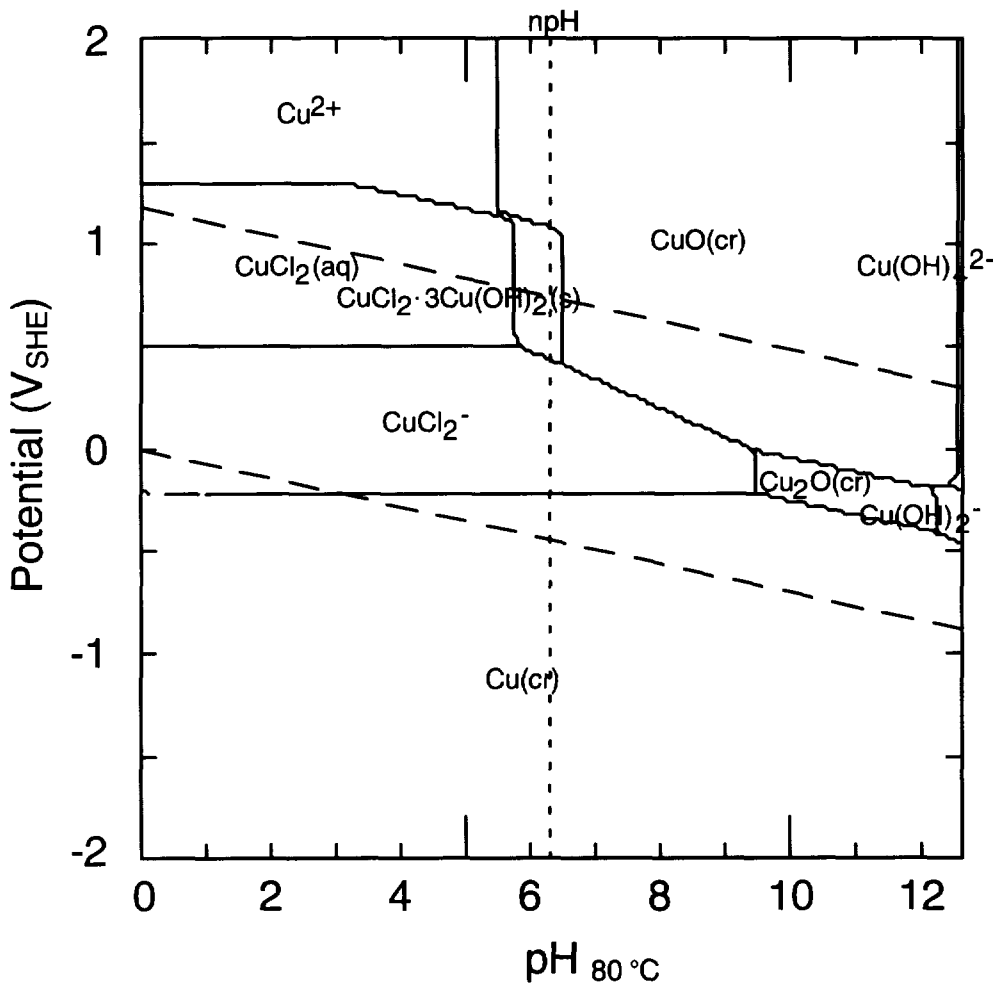


**Figure 7D**
Pourbaix diagram for copper species in the copper-chlorine-water system at 80 °C and $[Cu(aq)]_{tot} = 10^{-4}$ molal and $[Cl(aq)]_{tot} = 1.5$ molal.

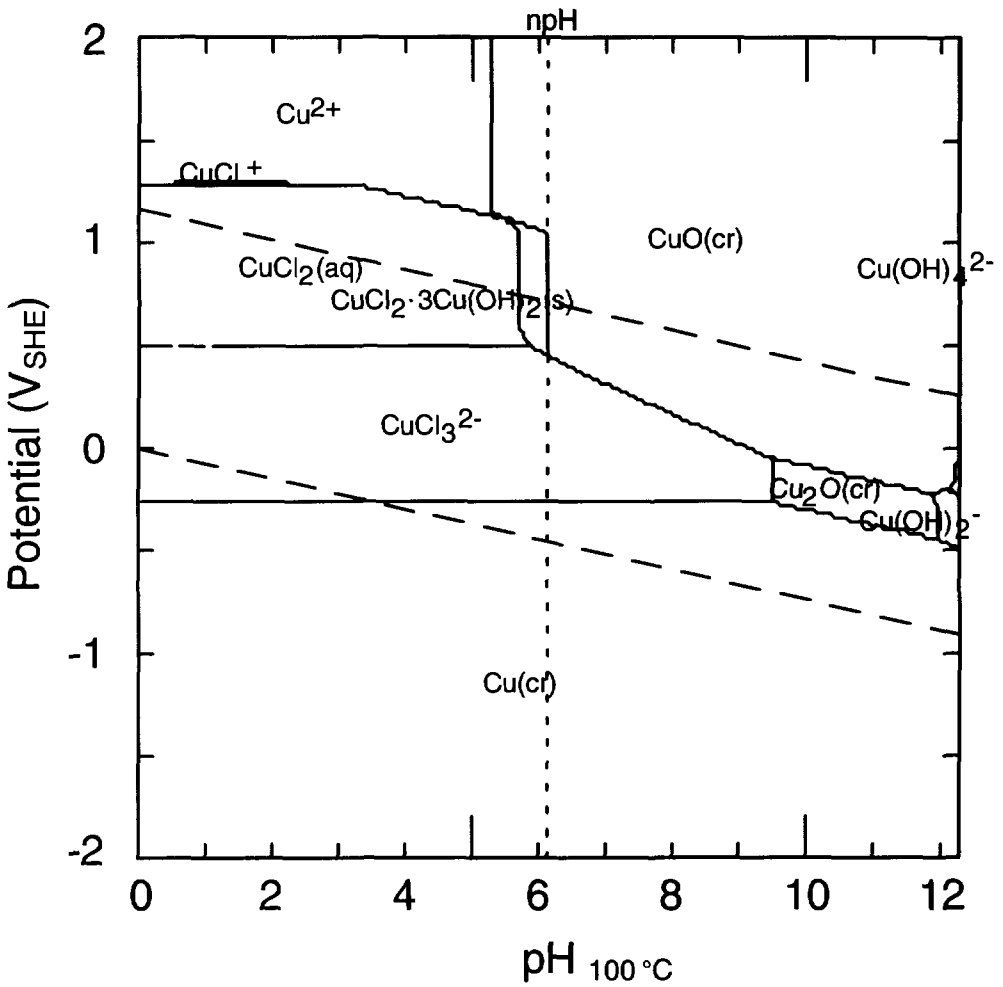


**Figure 7E**
Pourbaix diagram for copper species in the copper-chlorine-water system at 100 °C and $[Cu(aq)]_{tot} = 10^{-4}$ molal and $[Cl(aq)]_{tot} = 1.5$ molal.